Appendix VI

Detailed Blowdown/Washdown Transport Analysis for Pressurized-Water Reactor Volunteer Plant

VI.1 Introduction

In the event of a loss-of-coolant accident (LOCA) within the containment of a pressurized-water reactor (PWR), break-jet impingement will dislodge piping thermal insulation and other materials in the vicinity of the break. The steam/water flows induced by the break and containment sprays (CSs) will transport a fraction of this fragmented and dislodged insulation and other materials, such as chips of paint, paint particulates, and concrete dust, to the containment floor. Some of this debris eventually will transport to and will accumulate on the recirculation sump suction screens. Debris accumulation on the sump screen may challenge the sump's ability to provide adequate, long-term cooling water to the emergency core cooling system (ECCS) and to the CS pumps. The Generic Safety Issue (GSI)-191 study, "Assessment of Debris Accumulation on PWR Sump Performance," addresses the issue of debris generation, transport, and accumulation on the PWR sump screen and its subsequent impact on ECCS performance. The GSI-191 study examined whether debris accumulation in containment following a postulated LOCA would prevent or impede the performance of the ECCS. Los Alamos National Laboratory has been supporting the U.S. Nuclear Regulatory Commission (NRC) in the resolution of GSI-191.

Analytical studies were performed and small-scale experimental programs (NUREG/CR-6772, 2002; NUREG/CR-6773, 2002) were conducted to support the resolution of GSI-191. A parametric evaluation of the U.S. PWR plants demonstrated that potential sump-screen blockage was a plausible concern for operating PWRs (NUREG/CR-6762, Vol. 2, 2002). As part of the GSI-191 study, a U.S. PWR plant was volunteered and selected for a detailed analysis to develop and demonstrate a methodology for estimating the debris-transport fractions within PWR containments using plant-specific data. This report documents the blowdown and washdown transport portion of the study, describes the methodology, and provides an estimate for the transport of debris from its points of origin to the sump pool. The transport analysis consisted of (1) blowdown debris transport, where the effluences from a high-energy pipe break would destroy insulation near the break and then transport that debris throughout the containment, and (2) washdown debris transport caused by the operation of the CSs. Along the debris-transport pathways, substantial quantities of debris came into contact with containment structures and equipment where that debris could be retained, thereby preventing further transport. The blowdown/washdown debris-transport analysis provides the source term for the subsequent sump-pool debris-transport analysis.

The volunteer plant has a large, dry, cylindrical containment with a hemispherical dome constructed of steel-lined reinforced concrete and having a free volume of approximately 3 million ft^3. The nuclear steam supply system is a Westinghouse reactor with four steam generators (SGs). Each of the SGs is housed in a separate compartment that vents upward into the dome. Approximately two-thirds of the free space within the containment is located in the upper dome region, which is relatively free of equipment. The lower part of the containment is compartmentalized. The internal structures are

supported independently so that a circumferential gap exists between the internal structures and the steel containment liner. Numerous pathways, including the circumferential gap, interconnect the lower compartments. The CS system has spray train headers at four different levels; however, approximately 70 percent of the spray nozzles are located in the upper dome. The spray system does not spray some spaces in the lower levels; therefore, areas of significant size exist where debris washdown by the sprays would not occur. The sprays activate when the containment pressure exceeds 18.2 psig. If the sprays do not activate, debris washdown likely would be minimal. The insulation composition for the volunteer plant is approximately 13 percent fiberglass, 86 percent reflective metal insulation (RMI), and 1 percent Min-K insulation. For the purposes of this study, it was assumed that the fiberglass insulation was one of the low-density fiberglass (LDFG) types. For plant-specific analyses, these transport results for fibrous debris may have to be adjusted to compensate if the fiberglass insulation makeup is determined to be significantly different.

The effluences from a high-energy pipe break not only would destroy insulation near the break but also would transport that debris throughout the containment (i.e., blowdown debris transport). Substantial amounts of this airborne* debris would come into contact with containment structures and equipment and would be deposited onto these surfaces. As depressurization flows slow, debris would settle gravitationally onto equipment and floors. If pressurization of the containment were to occur, the CSs would activate to suppress pressurization. These sprays would tend to wash out remaining airborne debris (except in areas not covered by the sprays), and the impact of these sprays onto surfaces and the subsequent drainage of the accumulated water would wash deposited debris downward toward the sump pool (i.e., washdown debris transport). In addition, CSs could degrade certain types of insulation debris further through the process of erosion, thereby creating even more of the fine transportable debris.

An assessment of the likelihood of blocking the recirculation sump screens requires an estimate of the debris transport from the containment to the sump pool.† The debris transport within the sump pool is analyzed separately from this analysis, but the sump pool analysis requires the quantities of debris and the entry locations and timing as input to that analysis. This analysis sought to develop and demonstrate an effective methodology for estimating the transport of debris from the debris point of origin in the containment down to the sump pool, thereby providing the source term to the sump-pool debris-transport analysis. Applying the methodology to the volunteer plant generated plausible debris-transport fractions for that plant.

The analyses herein considered only one break location—a LOCA located in one of the SG compartments, which is a probable location for that plant because most of the primary system piping is located in these compartments.

Neither the debris-size distributions nor the overall transport fractions in this report are valid for plant-specific evaluations because these fractions were calculated using LOCA-generated debris-size distributions that did not account properly for PWR jet

* The terms “airborne” and “airflow” are used loosely with regard to gas flows, which actually consist of both air and steam.

† The simplest and most conservative assessment would be to assume 100-percent transport to the sump pool.

characteristics. Boiling-water reactor (BWR) jet characteristics were substituted for PWR jet characteristics because the PWR jet analyses had not yet been performed. When the PWR jet characteristics do become available, the overall transport fractions can be recalculated easily using PWR LOCA-generated debris-size characteristics.

The basic concepts of this methodology apply to the assessment of the debris transport within other PWR plants as well; however, that application depends on the plant-specific aspects of each plant. The complexity of a plant-specific methodology could vary significantly from one plant to the next.

VI.2 Debris-Transport Phenomenology

Both the spectrum of physical processes and phenomena and the features of a particular containment design would influence the transport of debris within a PWR. Because of the violent nature of flows following a LOCA, insulation destruction and subsequent debris transport are rather chaotic processes. For example, a piece of debris could be deposited directly near the sump screen or it could take a much more tortuous path, first going to the dome and then being washed back down to the sump by the sprays. Conversely, a piece of debris could be trapped in any number of locations. Aspects of debris-transport analysis include the characterization of the accident, the design and configuration of the plant, the generation of debris by the break flows, and both air- and water-borne debris dynamics.

Long-term recirculation cooling must operate according to the range of possible accident scenarios. A comprehensive debris-transport study should consider an appropriate selection of these scenarios, as well as all engineered safety features and plant-operating procedures. A small subset of accident scenarios will likely determine the maximum debris transport to the screen, but this scenario subset should be determined systematically. Many important debris-transport parameters will be dependent on the accident scenarios. These parameters include the timing of specific phases of the accident (i.e., blowdown, injection, and recirculation phases) and pumping flow rates. The blowdown phase refers to primary-system depressurization. The injection phase corresponds to ECCS injection into the primary system, a process that subsequently establishes the sump pool. The recirculation phase refers to long-term ECCS recirculation.

Many features in nuclear power plant containments significantly affect the transport of insulation debris. The dominant break flows will move from the break location toward the pressure suppression system (i.e., the suppression pool in BWR plants and the upper regions of the compartment in PWR plants). Structures such as gratings are placed in the paths of these dominant flows and likely would capture substantial quantities of debris. The lower compartment geometry (e.g., the open floor area, ledges, structures, and obstacles) defines the shape and depth of the sump pool and is important in determining the potential for debris to settle in the pool. Furthermore, the relative locations of the sump, LOCA break, and drainage paths from the upper regions to the sump pool are important in determining pool turbulence, which in turn determines whether debris can settle in the pool.

Transport of debris depends strongly on the characteristics of the debris that has formed. These characteristics include the types of debris (e.g., insulation type, coatings, and dust) and the size distribution and form of the debris. Each type of debris has its

own set of physical properties, such as densities, specific surface areas, buoyancy (including dry, wet, or partially wet), and settling velocities in water. The PWR plants use several distinct types of insulation (NUREG/CR-6762, Vol. 2, 2002). The size and form of the debris, in turn, depends on the method of debris formation (e.g., jet impingement, erosion, aging, and latent accumulation). The size and form of the debris affect whether the debris passes through a screen, as well as the transport of the debris to the screen. For example, fibrous debris may consist of individual fibers or of large sections of an insulation blanket and all sizes within these two extremes.

The complete range of thermal-hydraulic processes affects the transport of insulation debris, and the containment thermal-hydraulic response to a LOCA includes most forms of thermal-hydraulic processes. Debris transport is affected by a full spectrum of physical processes, including particle deposition and resuspension for airborne transport and both settling and resuspension within calm and turbulent water pools for both buoyant and nonbuoyant debris. The dominant debris-capture mechanism in a rapidly moving flow likely would be inertial capture; however, in slower flows, the dominant process likely would be gravitational settling. The CSs or possibly condensate drainage would likely wash off much of the debris deposited onto structures. Other debris on structures could be subject to erosion.

A panel of experts sought to identify and rank the important phenomena, processes, and systems with regard to PWR debris transport (LA-UR-99-3371, 1999). The analysis methodology incorporated the insights gained from the work of this panel. Additionally, this analysis accessed all of the experimental and analytical research performed to resolve the BWR strainer-blockage issue (LA-UR-01-1595, 2001; NUREG/CR-6369-1, 1999; NUREG/CR-6369-2, 1999; NUREG/CR-6369-3, 1999). The NRC published a summary on the base of knowledge for the effect of debris on PWR ECC sump performance (NUREG/CR-6808, 2003).

VI.3 Methodology

VI.3.1 Overall Description

Transport of LOCA-generated debris from its point of origin to the PWR sump pool is a multifaceted procedure involving many physical processes and complex plant-specific geometry. To evaluate the blowdown and washdown debris transport within the drywell of a BWR plant, the NRC developed a methodology that accomplished the objectives of the drywell debris-transport study (DDTS) (NUREG/CR-6369-1, 1999; NUREG/CR-6369-2, 1999; NUREG/CR-6369-3, 1999). The BWR methodology provided the basis for the methodology used herein.

The BWR methodology separated the overall transport problem into many smaller problems that were either amenable to the solution or that could be judged conservatively. The breakdown of the problem was organized using logic charts that were similar to well-known event-tree analyses. For some solution steps, sufficient data were available to solve that step reasonably. For other steps, insufficient data were available; therefore, the solution required the use of engineering judgment that was applied after review of the available knowledge base. Judgments were tempered to the desired level of conservatism called for in that particular analysis (sometimes assuming the worst case for a particular step). The result of each specific analysis was a transport fraction, defined as the fraction of insulation contained within the pipe-break destructive

zone of influence (ZOI) that subsequently was damaged or destroyed by a LOCA and was eventually transported to the suppression pool. Certainly, the degree of refinement that is feasible depends on available resources and time restraints. In addition, the conservatism in the estimates for each step in the divided problem may be compounded when the final transport fraction is quantified.

The PWR debris-transport methodology necessarily will differ from the BWR transport methodology because of differences in plant designs. These differences include the basic transport pathways, dominant capture mechanisms, and the timing of the accident sequence events. The dominant transport pathway for a PWR is different from the dominant pathway for a BWR. In a BWR, where pressure suppression would be caused by steam condensation in the suppression pool, the debris initially would be transported directly to the suppression pool, where the ECCS strainers operate. In PWR containments, which are designed to suppress pressurization by channeling break effluences* to the relatively large free volume of PWR containments, debris likely would be blown away from the sump area initially. Because one-half to three-quarters of the containment free volume typically is located in the upper regions of the containment, including the dome, it is justified to assume that a significant fraction of the small debris is blown directly into the upper regions, where the debris will settle onto floor surfaces or structures. Although the CSs could then wash the debris blown into the upper regions back down to the compartment sump area, the washdown pathway can be tortuous and could certainly result in substantial debris entrapment.

The dominant debris-capture locations are different in a PWR than in a BWR. In many typical PWRs, the likely dominant locations are the upper regions of the containment, the ice condensers in an ice-condenser plant, the refueling pool, an outer annulus pool, and the sump pool. In the volunteer-plant containments, dominant locations for debris capture may not exist; rather, the debris likely would be blown throughout the entire containment. Gratings in a PWR could play a substantially different role versus the gratings played in the BWR methodology because the debris likely would be blown up through a grating as opposed to down through a grating. Debris trapped underneath a grating would be less likely to remain there than debris trapped on top of a grating.

The water drainages of break recirculation overflow, the CSs, and condensate would cause debris transport during the washdown phase. The drainage of the activated CSs would be the most important of these drainages because the sprays usually cover a majority of the containment free volume, whereas the break overflow would wash only surfaces directly below the break. In a PWR, the break overflow could impinge on piping and equipment before reaching the containment sump floor, thereby washing debris from these surfaces, as well as potentially dispersing the flow. In a BWR, the break overflow for a majority of postulated breaks would pass down through at least one grating, where the flows would erode larger debris trapped on the gratings directly below the break—a situation less likely in a PWR. Although condensate drainage could transport debris from surfaces, the quantities of debris transported would likely be much less than the quantities transported by spray drainage.

The following methodology was designed specifically to analyze debris transport within the volunteer-plant containments; however, it also applies directly to several other

* In an ice-condenser plant, the break effluences would be channeled through the ice banks to condense steam.

containment designs, and it can be modified to tailor the methodology to any other PWR design. The best method for a particular plant will depend on the complexity of the containment design. If the containment has definitive upper and lower compartments that are separated by relatively few and narrow pathways, the analysis may be used to track debris transports in a manner similar to the DDTS analysis. Using an ice-condenser plant as an example, the containments were designed specifically to channel break flow through the ice banks to the dome region. This generally means that the connecting flow pathways between the lower and upper containments include the ice banks, small air-circulation return pathways (needed to establish postblowdown air circulation through the ice banks), and refueling-pool drains. Debris capture through the ice banks could be substantial. In addition, a large fraction of the small and fine debris would be blown into the dome region, where substantial quantities could be retained, even with the CSs operating.

The analysis here would focus on debris capture in the ice banks during blowdown and on debris retention in the upper compartment during the spray washdown process to identify debris transported from the lower containment and not likely to return there. Some plants would have a flooded outer annulus in which debris deposited in that pool would be less likely to transport from that pool to the sump pool. A conservative estimate of the maximum debris quantities that would be expected to transport to the sump pool can be made by subtracting masses of debris retained at various locations from the generation totals.

The design of the volunteer-plant containments is more complex than an ice-condenser design, from a debris-transport perspective; that is, the lower and upper regions of the containment are less well defined and are connected by several different pathways, thereby making it difficult to determine the motion of air and steam flows and the transport of debris. Certainly, system-level codes such as MELCOR can model the progression of break flows throughout the containment; however, the input model for the volunteer plant would have to be rather detailed to follow the flows through all of the lower levels in the containment. The modeling detail must include all of the levels and rooms and separate sprayed areas from nonsprayed areas. The model would need to simulate all of the connecting flow pathways, such as stairwells, equipment hatches, and doorways. The volunteer-plant analysis did not include a detailed thermal-hydraulics analysis.

The transport and deposition of insulation debris cannot be simulated realistically using a thermal-hydraulics computer code that incorporates aerosol transport models. Inertial capture serves as the primary mode of debris capture during the violent primary-system depressurization. The available models for inertial capture are based on data taken for rather simple geometries (e.g., a bend in a pipe). Current codes cannot reasonably model inertial capture in the complex geometry of containments. However, inertial capture can be determined in specific parts of the containment. For example, at the volunteer plant, the personnel access doors between an SG compartment and the sump annulus have at least one 90-degree bend. A LOCA, particularly a large LOCA, in an SG compartment would result in depressurization flows that would carry insulation debris through these doors with the flow. As the flow moved through the sharp bend, inertia would cause the deposition of some types of debris on the wall at the bend. The tests conducted at the Colorado Engineering Experiment Station, Inc. (CEESI) demonstrated an average inertial capture fraction for fibrous debris of 17 percent at such a bend if the surface were wetted, and analysis has shown that surfaces within the containment likely

would build a filmy layer of condensation rapidly. Because the CSs do not impinge on these wall surfaces, the debris would remain attached to those surfaces. In this situation, small amounts of debris can be removed from the equation, thereby lowering the transport fraction. Perhaps many of these types of definable captures can add up to a significant reduction in the transport fraction. Again, the size of that reduction would depend somewhat on both the geometry/conditions and the depth of the analysis.

The mechanics of this methodology basically involve looking for such reductions systematically. The demonstration of this methodology in this volunteer-plant analysis assumed a large LOCA occurred inside SG compartment number 1 (SG1) of the containment. Figure VI-1 illustrates this methodology in the general sense. First, the blowdown dispersal of the debris is estimated until all of the debris is associated with some surface area. Then the likelihood of debris remaining on each of these surfaces during washdown is estimated or judged. For example, debris deposited onto a surface that has been impacted by the CSs is much more likely to transport than debris deposited onto surfaces that have been wetted only by condensate.

As with the DDTS, the debris for transport must first be categorized according to type and size according to transport properties so that the transport of each type of debris can be analyzed independently. Some damage is assumed for all insulation located within the break-region ZOI. Section VI.3.2 discusses these categories and their properties.

The containment free volume in the volunteer plant was subdivided into many regions based on geometry and the locations of the CSs. The volume region containing the postulated LOCA was analyzed first. For SG1, a MELCOR simulation of only the break compartment determined the distribution of flows exiting that compartment (i.e., the fraction of flow going upward into the dome as opposed to the fraction entering the lower levels through personnel access doors). Debris capture within SG1 was based on such considerations as flows through gratings and flows making sharp bends (see Section VI.3.3.1). In each region, debris capture would deposit debris onto the floor or other surfaces, based on surface areas and judgment regarding whether debris was deposited by settling or by another mechanism. The analysis treated floor surfaces separately because these surfaces would collect and drain spray water differently from vertical surfaces, for example, and because debris that gravitationally settles would deposit onto horizontal surfaces. These surfaces were divided further according to their exposure to spray and condensate moisture. All surfaces would collect condensate. The sprays would impact some surfaces directly, and others simply would be washed by the process of spray drainage. Debris entrained by spray-drainage water could become captured a second time as the drainage fell from one level to another.
Because the chart illustrated in Figure VI-1 would become unreasonably large if it were developed for the entire volunteer-plant containment, another approach was used. The process was handled using an equation-format model (described in Figure VI-1), with the input entered into data arrays.

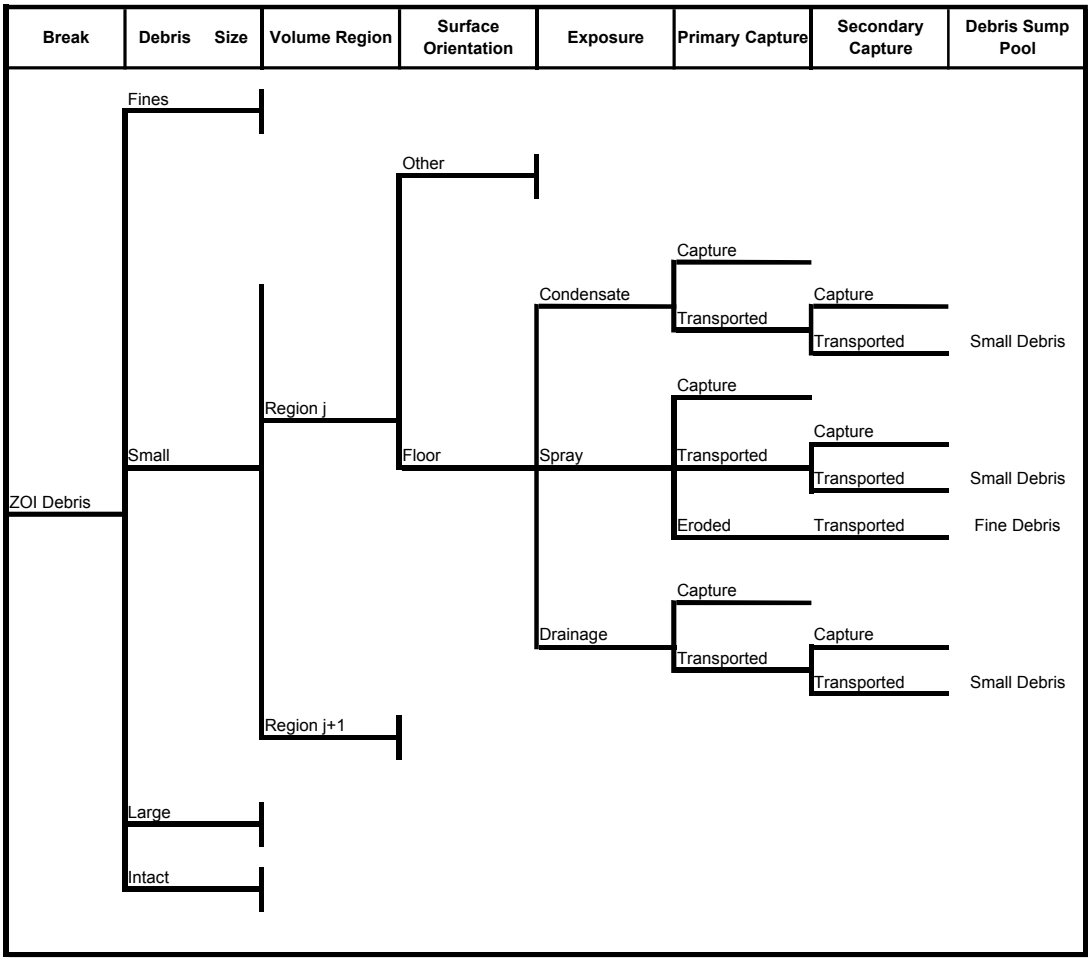

Figure VI-1. Example of a Section of a Debris-Transport Chart

VI.3.2 Debris-Size Categorization

The types of insulation used inside the volunteer-plant containments include fiberglass insulation,* RMI, and stainless-steel-encapsulated Min-K insulation at approximately 13.4 percent, 85.7 percent, and 0.9 percent, respectively (NUREG/CR-6762, Vol. 2, 2002). Although RMI comprises a majority of the insulation within these containments, the fibrous insulation more likely would cause blockage of the sump. First, the RMI debris would transport less easily than the fibrous debris (i.e., it takes a faster flow of water to move RMI debris than it does for fibrous debris). In addition, it takes substantially more RMI debris than fibrous debris on the sump screens to block the flow effectively through the screens. Although the Min-K debris, in combination with the fibrous debris, could create substantial head losses on the screen, the inventory of the Min-K in the containments is relatively low. Therefore, this analysis focused primarily on the transport of fibrous debris, with the transport of RMI and Min-K estimated more crudely.

* The type (or types) of fiberglass insulation used in the volunteer-plant containments has yet to be determined. This analysis assumes that the fiberglass is LDFG.

The difficulties associated with determining debris-size distributions to represent the LOCA-generated debris are (1) the limited debris-generation data and (2) the need to determine the characteristics of the LOCA jet (i.e., the size of the ZOI and volumes within specific pressure isobars). The limitations in the debris-generation data must be handled by skewing the integration of size fractions conservatively over the ZOI toward the smaller debris sizes—the more limited the data, the more conservative the integration. The determination of the jet characteristics for a PWR jet is a relatively straightforward analysis, but those characteristics unfortunately were not yet available for use in this report. Because debris-size distributions are necessary to determine estimates for the overall transport of debris to the sump pool, assumptions were made to provide distributions that were suitable to illustrate the transport methodology.

Therefore, neither the debris-size distributions nor the overall transport fractions in this report are valid for plant-specific evaluations.

However, the transport fractions for specific debris-size classes are considered to be valid for the volunteer plant.

VI.3.2.1 Fibrous Insulation Debris-Size Categorization

The analysis assumed some damage to all insulation located within the break-region ZOI. The damage could range from slight damage (insulation erosion occurring through a rip in the blanket cover) that leaves the blanket attached to its piping to the total destruction of a blanket (with its insulation reduced to small or very fine debris). This analysis considered all of the insulation within the ZOI to be debris. The fibrous debris was categorized into one of four categories based on transport properties so that the transport of each type of debris could be analyzed independently. Table VI-1 shows these categories and their properties.

The two smaller and two larger categories differed primarily as to whether the debris was likely to pass through a grating that is typical of those found in nuclear power plants. The DDTS analysis also used this criterion. Thus, fines and small pieces pass through gratings but large and intact pieces do not. The fines and small pieces are much more transportable than the large debris. The fines were then distinguished from the small pieces because the fines would tend to remain in suspension in the sump pool, even under relatively quiescent conditions, whereas the small pieces would tend to sink. Furthermore, the fines tended to transport slightly more as an aerosol in the containment-air/steam flows and were slower to settle than the small pieces when airflow turbulence decreased. The CEESI tests illustrated that when an LDFG blanket was completely destroyed, 15 to 25 percent of the insulation was in the form of very fine debris (i.e., debris too fine to collect readily by hand).

Table VI-1. Debris-Size Categories and Their Capture and Retention Properties

Fraction Variable	Size	Description	Airborne Behavior	Waterborne Behavior	Debris-Capture Mechanisms	Requirements for Crediting Retention
D_F	Fines	Individual fibers or small groups of fibers.	Readily moves with airflows and slow to settle out of air, even after completion of blowdown.	Easily remains suspended in water, even relatively quiescent water.	Inertial impaction Diffusiophoresis Diffusion Gravitational settling Spray washout	Must be deposited onto surface that is not subsequently subjected to CSs or to spray drainage. Natural-circulation airflow likely will transport residual airborne debris into a sprayed region. Retention in quiescent pools without significant flow through the pool may be possible.
D_S	Small Pieces	Pieces of debris that easily pass through gratings.	Readily moves with depressurization airflows and tends to settle out when airflows slow.	Readily sinks in hot water, then transports along the floor when flow velocities and pool turbulence are sufficient. Subject to subsequent erosion by flow water and by turbulent pool agitation.	Inertial impaction Gravitational settling Spray washout	Must be deposited onto surface that is not subsequently subjected to high rates of CSs or to substantial drainage of spray water. Retention in quiescent pools (e.g., reactor cavity). Subject to subsequent erosion.

Fraction Variable	Size	Description	Airborne Behavior	Waterborne Behavior	Debris-Capture Mechanisms	Requirements for Crediting Retention
D_L	Large Pieces	Pieces of debris that do not easily pass through gratings.	Transports with dynamic depressurization flows but generally is stopped by gratings.	Readily sinks in hot water and can transport along the floor at faster flow velocities. Subject to subsequent erosion by flow water and by turbulent pool agitation.	Trapped by structures (e.g., gratings) Gravitational settling	Must be either firmly captured by structure or on a floor where spray drainage and/or pool flow velocities are not sufficient to move the object. Subject to subsequent erosion.
D_I	Intact	Damaged but relatively intact pillows.	Transports with dynamic depressurization flows, stopped by a grating, or may even remain attached to its piping.	Readily sinks in hot water and can transport along the floor at faster flow velocities. Assumed to remain encased in its cover, thereby not subject to significant subsequent erosion by flow water and by turbulent pool agitation.	Trapped by structures (e.g., gratings) Gravitational settling Not detached from piping	Must be either firmly captured by structure or on a floor where spray drainage and/or pool flow velocities are not sufficient to move the object. Intact debris subsequently would not erode because of its encasement.

The distinguishing difference between the large and intact debris was whether the blanket covering still protected the fibrous insulation, and therefore whether the CSs could further erode the insulation material.

The analysis first estimated the volume (or mass) distribution, D_i, of the four categories of insulation debris. This estimate assumed that the fibrous insulation within the ZOI was uniformly distributed and that the distribution must add up to one, as

$$\sum_{i=1}^{N_{types}} D_i = 1 \quad ,$$

where

D_i = the fraction of total debris that is type *i*.

The volume of each category of debris is simply the distribution fraction multiplied by the total volume of insulation within the ZOI. Debris-transport analysis has used volumes of fibrous debris interchangeably with mass on the basis that the density is that of the undamaged (as fabricated) insulation. Certainly the density would be altered by the destruction of the insulation and again when the debris became water saturated. For example, the physical volume of debris on the screen must include the actual density of the debris on the screen as

$$V_i = D_i V_{ZOI} \quad ,$$

where

V_i = the volume of debris of type *i* and

V_{ZOI} = the total volume of insulation contained within the ZOI.

The estimation of the debris-size distribution must be based on experimental data. When sufficient data are available, the following analytical model illustrates how the fraction of fine and small debris can be estimated from that data. Using the spherical ZOI destruction model, the fraction of the ZOI insulation that becomes type-*i* debris is given by

$$F_i = \frac{3}{r_{ZOI}^3} \int_0^{r_{ZOI}} g_i(r)\, r^2 \, dr \quad ,$$

where

F_i = the fraction of debris of type *I*,

$g_i(r)$ = the radial destruction distribution for debris of type *I*,

r = the radius from the break in the spherical ZOI model, and

r_{ZOI} = the outer radius of the ZOI.

Typical test data provide an estimate of the damage to insulation samples at selected distances from the test jet nozzle (i.e., the size distribution of the resultant debris). The jet pressure at the target is determined from test pressure measurements, suitable analytical models, or both. Thus, the size distribution as a function of the jet pressure is obtained. The volume associated with a particular level of destruction is determined by estimating the volume within a particular pressure isobar within the jet (i.e., any insulation located within this pressure isobar would be damaged to the extent (or greater) associated with that pressure). The isobar volumes then are converted to the equivalent spherical volumes; thus, the debris-size distribution is associated with the spherical radius (i.e., $g_i(r)$). The distribution would be specific to a particular kind of insulation, jacketing, jacketing seam orientation, and banding.

To demonstrate the transport methodology completely, the analysis assumed that the volunteer-plant containments used LDFG insulation as the fibrous insulation, since significant data on LDFG insulation are available to predict the LOCA-generated size distribution. The most extensive debris-generation data for LDFG insulation are the data from the BWR Owners Group (BWROG) air-jet impact tests (AJITs) (NEDO-32686, 1996). These data, combined with the jet characteristics of a PWR LOCA, could result in a realistic LOCA size distribution; however, the PWR jet characteristics were not available at the time of this writing.

The development of a suitable size distribution for the purposes of demonstrating this methodology follows. For fibrous debris, the BWROG correlated the fraction of the original insulation that became fine debris with the distance from the jet nozzle and then crudely estimated the ZOI destruction fractions for specific types of insulation. The fine debris in the BWROG analysis correlates with the combined fine and small debris of Table VI-1.

For the NUKON™ insulation debris—both jacketed and unjacketed insulation—the BWROG recommended in its utility resolution guidance (URG) the assumption that 23 percent of the insulation within the ZOI be considered in the strainer head-loss evaluations during the resolution of the BWR strainer-blockage issue. Applying this recommendation to this analysis means that 23 percent of the ZOI would be distributed between the fine and small debris and that the remaining 77 percent would be distributed between the large and intact debris. The NRC reviewed the BWROG recommendations and documented its findings in a safety evaluation report (SER) (NRC-SER-URG, 1998). Although the NRC had some reservations regarding the BWROG's method for determining the debris fractions, the NRC believed the debris fractions to be conservative primarily because the blanket seams were arranged in the AJITs to maximize the destruction of the blankets.

Whereas the BWROG based its recommendations on AJITs, more recent testing using two-phase jet impact testing indicated the need for somewhat higher small-debris fractions than did the AJIT data (refer to Section 3.4.2.2 in this SER for the evaluation of the two-phase jet concern). Ontario Power Generation (OPG) of Canada conducted these debris-generation tests (OPG, 2001). A report (NUREG/CR-6762, Vol. 3, 2002)

supporting the PWR parametric evaluation (NUREG/CR-6762, Vol. 1, 2002) compared the AJIT and the OPG tests. This comparison illustrated the potential for a two-phase jet to generate more small debris than the AJIT data indicated. The parametric evaluation concluded when comparing these two sets of test data the small debris fraction should be increased from the BWROG recommendation. The evaluation used engineering judgment to increase the recommended destruction fraction for small debris from 23 percent to 33 percent. The remaining 67 percent of the insulation would be assumed to be large debris either exposed or enclosed in its covering material.

This analysis split the small-debris fraction of 33 percent that was used in the parametric evaluation to accommodate the fine- and small-debris categories of this analysis. The analysis of the AJIT testing performed at CEESI to support the DDTS determined that whenever entire blankets were completely destroyed, 15 to 25 percent of the insulation was too fine to collect by hand.* In this case, complete destruction means that nearly all of the insulation was either fine or small pieces. In any case, 15 to 25 percent of the blanket (an average of 20 percent) can be considered fine debris for the purposes of this analysis. This analysis assumed that 20 percent of the 33-percent small-debris fraction was fine debris (i.e., $0.2 \times 0.33 = 0.066$). Therefore, the analysis estimated the destruction of 7 percent of the ZOI insulation into fine debris, leaving 26 percent for the small-piece debris.

In a similar manner, this analysis split the parametric evaluation of the 67-percent large-debris fraction to accommodate the large- and intact-debris categories. The DDTS analysis, based on the AJIT data, assumed that 40 percent of the blanket insulation remained covered. This analysis accepted the DDTS assumption of 40 percent for the covered (intact) debris fraction. However, that number had to be adjusted downward to account for the increase in the small-debris fraction from 23 to 33 percent (i.e., $0.67/0.77 \times 0.4 = 0.35$). Therefore, 35 percent of the ZOI insulation was considered to be intact debris, leaving 32 percent for the exposed large-piece debris. Table VI-2 summarizes the debris category distribution for fibrous debris assumed in this analysis.

Table VI-2. Fibrous-Debris Category Distribution

Category	Category Percentage
Fines	7%
Small Pieces	26%
Large Pieces	32%
Intact	35%

* This debris either was blown through the fine-mesh screen at the end of the test chamber and lost from the facility or was deposited onto surfaces inside the chamber in such a dispersed manner that it could be collected only by hosing down the walls and structures.

VI.3.2.2 RMI Insulation Debris-Size Categorization

In the volunteer-plant containments, the RMI insulation is made of stainless steel. Transco Products, Inc., manufactured the insulation around the reactor vessel. Diamond Power Specialty Company (DPSC) manufactured all of the other RMI inside the containments and marketed it as DPSC MIRROR™ insulation. Furthermore, the insulation panels generally are held in place simply by buckling the panels together (i.e., an absence of bands on most panels). Because the reactor vessel insulation is shielded from a postulated jet impingement for the most part, LOCA-generated RMI debris would consist primarily of the DPSC type. The BWROG (NEDO-32686, 1996) estimated, and the NRC accepted (NRC-SER-URG, 1998), the threshold jet-impingement pressure required to damage DPSC MIRROR™ insulation with standard bands as 4 psi; these data should be applicable to the volunteer-plant RMI. Therefore, some debris could be formed from any insulation subjected to a differential of 4 psi or greater, but the extent of damage would depend on the magnitude of the pressure. Insulation that is closer to the break would be destroyed completely and form small pieces of debris, whereas insulation farther from the break may remain nearly intact. The transport analysis requires a size distribution. Data from two experimental programs provide limited information on the extent of destruction that would occur in this type of RMI insulation. These programs are (1) the Siemens Karlstein tests (SEA-95-970-01-A:2, 1996) and (2) the BWROG AJIT (NEDO-32686, 1996).

Swedish Nuclear Utilities conducted metallic insulation jet impact tests at the Siemens AG Power Generation Group (KWU) test facility in Karlstein am Main, Germany, in 1994 and 1995. During this test program, the NRC conducted a single RMI debris-generation test to obtain debris-generation data and debris samples that are representative of RMI used in U.S. plants. The DPSC provided the NRC test sample. The NRC-sponsored test was performed with a high-pressure blast of two-phase water/steam flow from a pressurized vessel connected to a target mount by a blowdown line with a double-rupture disk. The target was mounted directly on a device designed to simulate a double-ended guillotine break (DEGB) such that the discharge impinged the inner surface of the RMI target as it would an insulation cassette surrounding a postulated pipe break. Most of the RMI debris was recovered and analyzed with respect to size distribution. Figure VI-2 shows the overall size distribution for the total recovered debris mass, and Figure VI-3 shows a photograph of the recovered RMI debris. This debris sample is likely typical of debris formed from the RMI cassettes nearest the break.

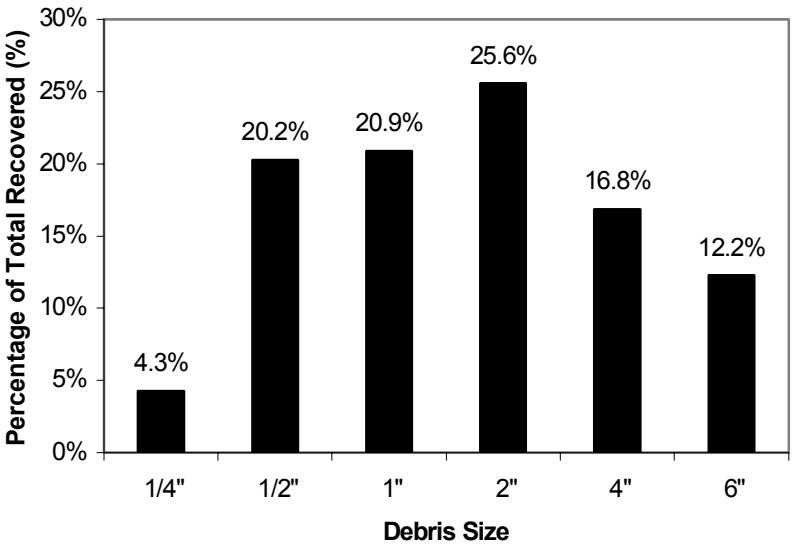

Figure VI-2. Size Distribution of Recovered RMI Debris

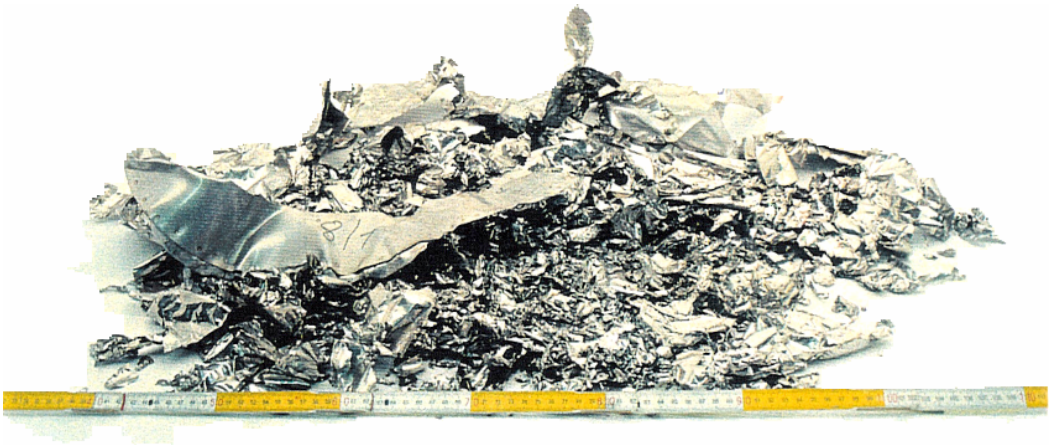

Figure VI-3. RMI Debris Observed in Siemens Steam-Jet Impact Tests

The BWROG-sponsored tests conducted at CEESI examined the failure characteristics of various types of insulation materials when subjected to jet impingement forces. The CEESI has compressed-air facilities that provided choked nozzle airflow. The tests directed this airflow at insulation samples mounted inside a test chamber that did not pressurize significantly but retained most of the insulation debris for subsequent analysis. The variety of insulation materials tested included samples of the stainless-steel DPSC MIRROR™ insulation. The test samples were mounted at various distances from the nozzle, thereby subjecting similar samples to varying damage pressures. In this manner, the test data were used to estimate the threshold pressure required to damage this type of insulation. The data also provided information regarding the size distribution of the resulting debris. The formation of debris depended on the separation of the outer sheath, which in turn depended on the type, number, and placement of the supporting bands. The data used herein were for stainless-steel DPSC MIRROR™ cassettes mounted either with standard bands or without bands; therefore, these data

are conservative with respect to data for cassettes mounted with even stronger banding. The recorded debris-generation data separated the quantities of debris into several distinct size groupings. For this transport analysis, the debris was grouped into three size groups: (1) debris generally smaller than 2 in., (2) debris larger than 2 in. but smaller than 6 in., and (3) all RMI pieces larger than 6 in. (including both debris and relatively intact insulation cassettes). Figure VI-4 shows the fractions of the collected debris for the two finer groups as a function of the damage pressure on the cassette; all other insulation either remained relatively intact or formed debris larger than approximately 6 in.

The BWROG data describe the damage to stainless-steel DPSC MIRROR™ insulation (standard banding) when subjected to jet pressures of up to 120 psi. The NRC-sponsored Siemens test demonstrates the complete destruction of stainless-steel DPSC MIRROR™ insulation when impacted by the highest jet pressure near the break. A gap exists in the data between 120 psi and the higher pressure near the jet. The damage to the RMI within the ZOI was estimated using the spherical equivalent volume method in conjunction with BWR-specific data (i.e., volumes with specific pressure isobars). The BWROG analysis that was provided to the utilities (NEDO-32686, 1996) was used to convert jet isobar volumes to equivalent spherical volumes. Furthermore, the outer radius of the equivalent sphere was assumed to be 12D (i.e., 12 times the diameter of the pipe break), which corresponds to an insulation destruction pressure of 4 psi for a BWR radial offset DEGB. **The resultant size distribution can demonstrate the overall transport methodology fully but is not suitable for PWR plant-specific analyses.** The BWROG data were applied when the impact pressure was less than 120 psi; the Siemens data were conservatively applied when the impact pressure was greater than 130 psi (insulation totally destroyed), and a linear extrapolation was applied between 120 and 130 psi. The data shown in Figure VI-4indicate that when the insulation is totally destroyed, approximately 70 percent of the debris would be less than approximately 2 in. in size and the remaining 30 percent would be between 2 and 6 in. in size.

Because of variability and uncertainty in debris-generation estimates, as well as the use of BWR-specific jet characteristics, it is prudent to enhance the fractions for the finer groups of debris, noting that the smaller debris would transport more easily than would the larger debris. One uncertainty is the fact that the BWROG data were generated using an air jet, whereas the postulated accident would involve a two-phase steam/water jet; the comparison of two-phase and air test data has indicated that a two-phase jet could generate finer debris than could an air jet. To make the debris-generation estimates more conservative to compensate for variability and uncertainty in the estimates, the fractions for the two fines size groups were increased by 50 percent. Table VI-3 shows the spherical volume damage estimates with and without the 50-percent increase.

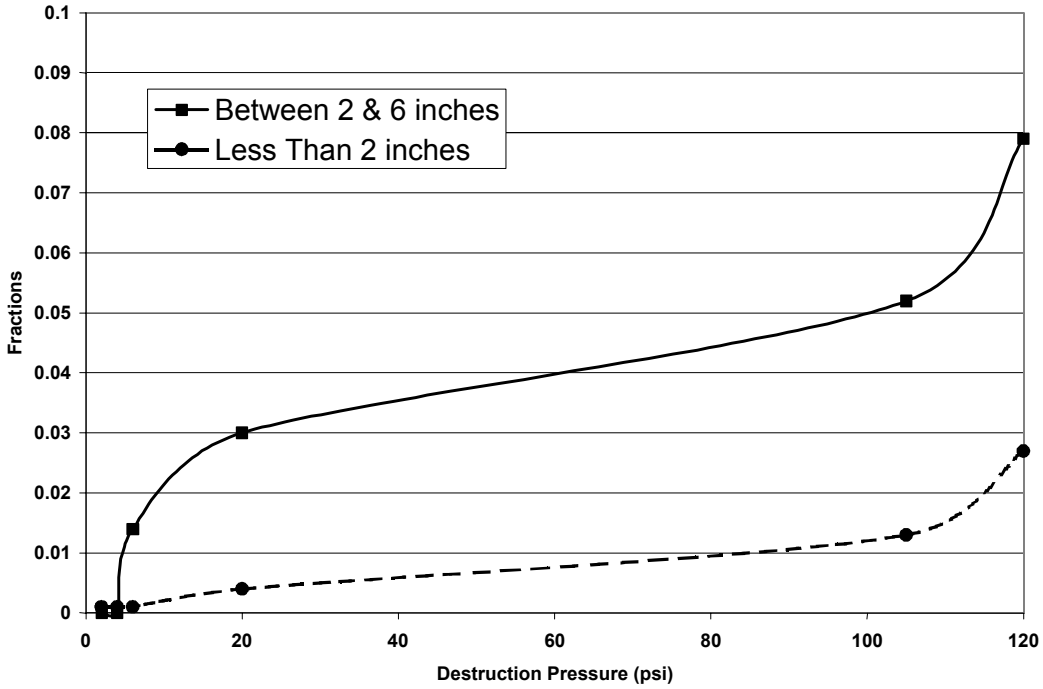

Figure VI-4. Relative Damage of Stainless-Steel DPSC MIRROR™ Insulation

Table VI-3. RMI Debris Category Distribution

Category	Category Percentage	
	Integration Result	Conservative Estimate
Less than 2 in.	14 percent	21 percent
Between 2 and 6 in.	8 percent	12 percent
Greater than 6 in.	78 percent	67 percent

VI.3.2.3 Min-K Insulation Debris-Size Categorization

In locations where insulation thickness was a specific concern, such as pipe-whip-restraint locations, fully encapsulated Min-K insulation was used instead of the usual RMI insulation. Containment-wide, approximately 0.9 percent of the insulation is Min-K. Although the potential quantities of Min-K debris would be substantially smaller than corresponding quantities of fibrous or RMI debris, a small amount of Min-K particulate debris could contribute more significantly than RMI debris to sump-screen head loss. In particular, Min-K debris dust would contribute to the particulate load in the debris bed when combined with the fibrous debris on the screens. Min-K is a thermo-ceramic insulation (also referred to as a particulate insulation) that is made of microporous material. The particulate insulations include calcium silicate, asbestos, Unibestos, Microtherm, and gypsum board. Test data have demonstrated that microporous particulate, combined with fibrous debris, creates a debris bed that can cause relatively high head losses across that bed. This head loss is over and above the corresponding

head loss associated with more ordinary particulate, such as corrosion products. The most notable of the particulate insulation types has been calcium silicate.

Limited debris-generation data exist for the microporous insulations, and most of the available data were obtained for calcium silicate. No debris-generation data were available for Min-K insulation. Data from tests conducted by the OPG (NUREG/CR-6762, Vol. 3, 2002) serve as the primary source of calcium silicate debris-generation data. These tests involved impacting aluminum-jacketed calcium silicate insulation targets with a two-phase water/steam jet. Figure VI-4 shows the size distribution data.

Even if it is assumed that Min-K behaves similarly to calcium silicate with regard to debris generation, the OPG data cover only a limited range of damage pressures. Integrating the damage over the spherical ZOI requires a conservative extrapolation to a full range of pressures. The ZOI for Min-K corresponds to a destruction pressure of 4 psi, based on the BWROG guidance to utilities. At high pressures, the conservative extrapolation should assume that complete destruction of the insulation occurs (i.e., all of the insulation is pulverized to dust). At lower pressures, the damage fractions of the lowest pressures tested would extend out to the ZOI boundary. This crude conservative extrapolation indicates that about half of the insulation should be considered dust. In addition to the conservative extrapolation, the debris-generation fraction is conservative with respect to the jacket seam angle relative to the jet. The seams in the test data shown in Figure VI-5 were oriented toward maximum damage. In reality, the seams within the ZOI likely would be distributed more randomly with respect to the jet; therefore, many of the jackets would provide more protection for the Min-K than the OPG data indicate. On the other hand, applying data for calcium silicate to Min-K insulation introduces substantial uncertainty.

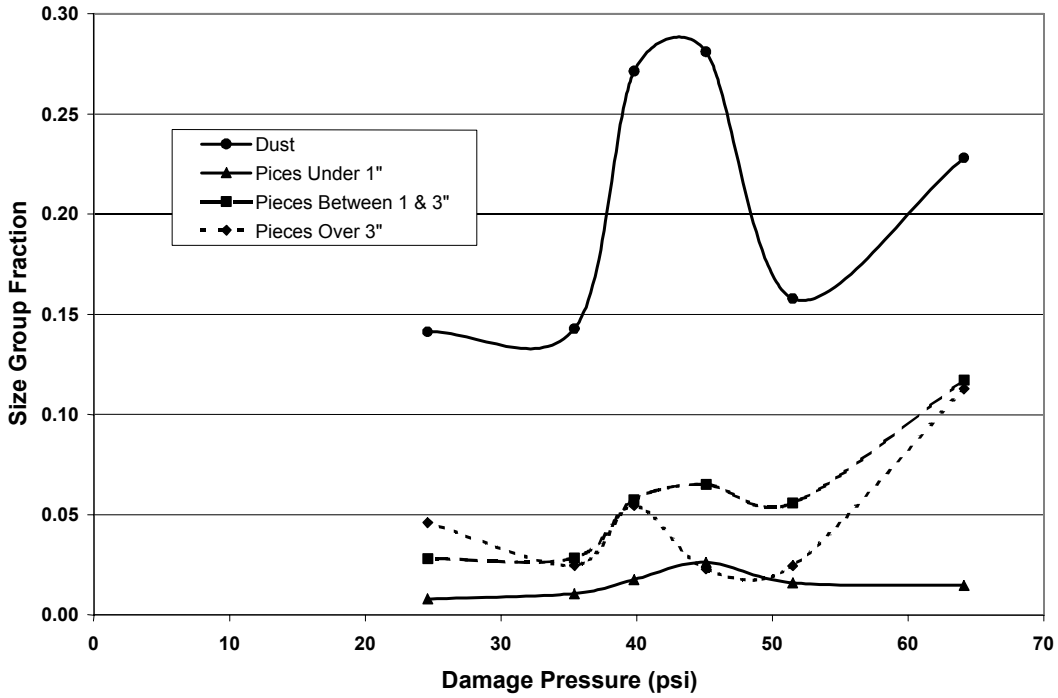

Figure VI-5. Debris-Size Distributions for OPG Calcium Silicate Tests

Another source of uncertainty is the location of the minimal quantities of Min-K insulation with respect to the break. A key assumption of the ZOI integration is a uniform distribution of insulation within the ZOI. However, with so little Min-K insulation inside the volunteer-plant containments, all damaged Min-K insulation could be located preferentially near or far from the break. Therefore, all Min-K insulation could be destroyed totally or only slightly damaged. Another source of uncertainty that has not been assessed experimentally is the subsequent erosion of the Min-K debris by the CSs. In light of these uncertainties, it is conservative and prudent to assume that all of the Min-K insulation inside a ZOI would be pulverized to dust.

VI.3.3 Blowdown Debris Transport

The break region, SG1, would be the source of all insulation debris and would be subject to the most violent of the containment flows, and the primary debris capture mechanism in this region would be inertial capture. For these reasons, the transport of debris within the region of the pipe break should be solved separately from that of the rest of the containment. The methodology is described for fibrous-debris transport but also was applied to RMI debris in a similar manner.

VI.3.3.1 Break-Region Dispersion and Capture

The first step in determining the dispersal of debris near the debris-generation source was to determine the distribution of the break flow from the region—specifically, the fractions of the flow directed to the dome versus other locations. This determination was accomplished using the containment thermal-hydraulics code MELCOR. The containment was designed to force reactor coolant system break effluents upward through the open tops of the SG compartments and into the dome. Figure VI-6 shows the nodalization diagram for the break-region MELCOR calculation.

The LOCA-generated debris that was not captured within the region of the break would be carried away from the break region by the break flows. The primary capture mechanism near the break would be inertial capture or entrapment by a structure such as a grating. The break-region flow that occurred immediately after the initiation of the break would be much too violent to allow debris simply to settle to the floor of the region.

The inertial capture of fine and small debris occurs when a flow changes directions, such as flows through the doorways from the SG compartments into the sump-level annular space. These flows must make at least one 90-degree bend through these doorways, and steam condensation as well as the liquid portion of the break effluence would wet these surfaces. Debris-transport experiments conducted at CEESI (NUREG/CR-6369-2, 1999) demonstrated an average capture fraction of 17 percent for fine debris and small debris that make a 90-degree bend at a wetted surface. Other bends in the flow would occur as the break effluents interacted with equipment and walls.

The platform gratings within the SG compartments would capture substantial debris, even though the gratings do not extend across the entire compartment. The CEESI debris-transport tests demonstrated that an average of 28 percent of the fine and small debris was captured when the airflow passed through the first wetted grating that it encountered and that an average of 24 percent was captured at the second grating. A grating would completely trap the large and intact debris. In addition, equipment such as beams and pipes was shown to capture fine and small debris. In the CEESI tests, the

structural maze in the test section captured an average of 9 percent of the debris passing through the maze.

To evaluate the transport and capture within the break region, the evaluation must be separated into many smaller problems that are amenable to resolution. This separation can be accomplished using a logic-chart approach that is similar to the approach developed for the resolution of the BWR-strainer-blockage issue (NUREG/CR-6369-1, 1999). Figure VI-7 shows the chart for a LOCA in the volunteer-plant SG1, which is based on the MELCOR nodalization diagram in Figure VI-6. This chart tracks the progress of small debris from the pipe break (Volume V12) until the debris is assumed to be captured or is transported beyond the compartment. Because SGs 1 and 4 are joined at two locations, the compartments were combined into one model (i.e., a LOCA in SG1 will discharge to the containment through SG4 as well).

The questions across the top of the chart, shown in Figure VI-7, alternate among volume capture, flow split, and junction capture as the debris-transport process progresses through the nodalization scheme. The nodalization scheme was constructed to place the gratings at junction boundaries. The first chart question (header) after the initiator asks how much debris would be captured in Volume V12, where the LOCA was postulated to occur. The evaluation of this question involves simply estimating the fraction of small debris that was deposited by inertia near the pipe break; the remainder of the debris would be assumed to transport beyond this volume. The next question in the chart concerns a flow split (i.e., the distribution of the break flow going upward or downward from the break). The flow split is actually a debris split (i.e., how much debris goes in each direction). For fine- and small-piece debris, it is reasonable to assume that the debris split is approximated by the flow split. For large and intact-piece debris, the debris split may differ from the flow split, depending on the geometry. The third question concerns the amount of the debris captured at the flow junction between two volumes. The two junctions in the third question represent gratings that extend partly across the compartment at two levels. The fourth question starts the cycle over again for the next set of volumes in the sequence.

Once the distributions are inserted into the chart and the results are quantified, the results will indicate the distribution of captured debris within the compartments, as well as the debris transport from the compartments. The chart also will indicate the destination of the debris that is transported from the SG compartments (e.g., the dome or the lower levels through access doorways).

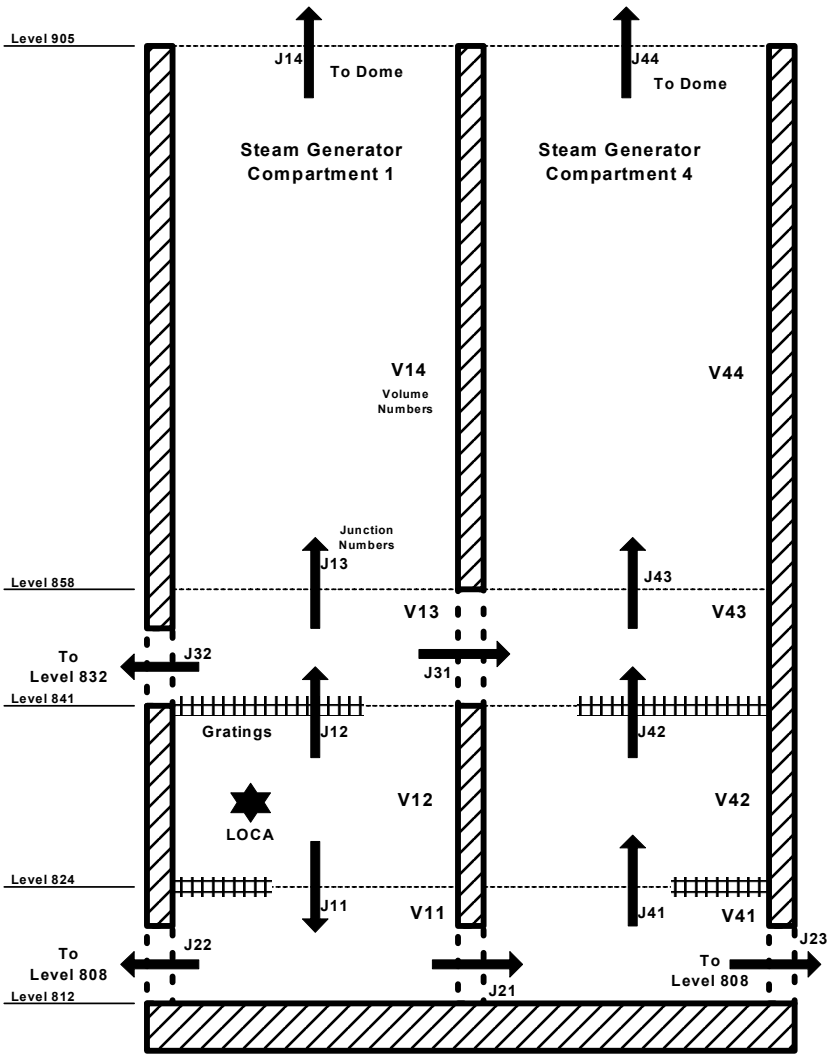

Figure VI-6. Break-Region Nodalization

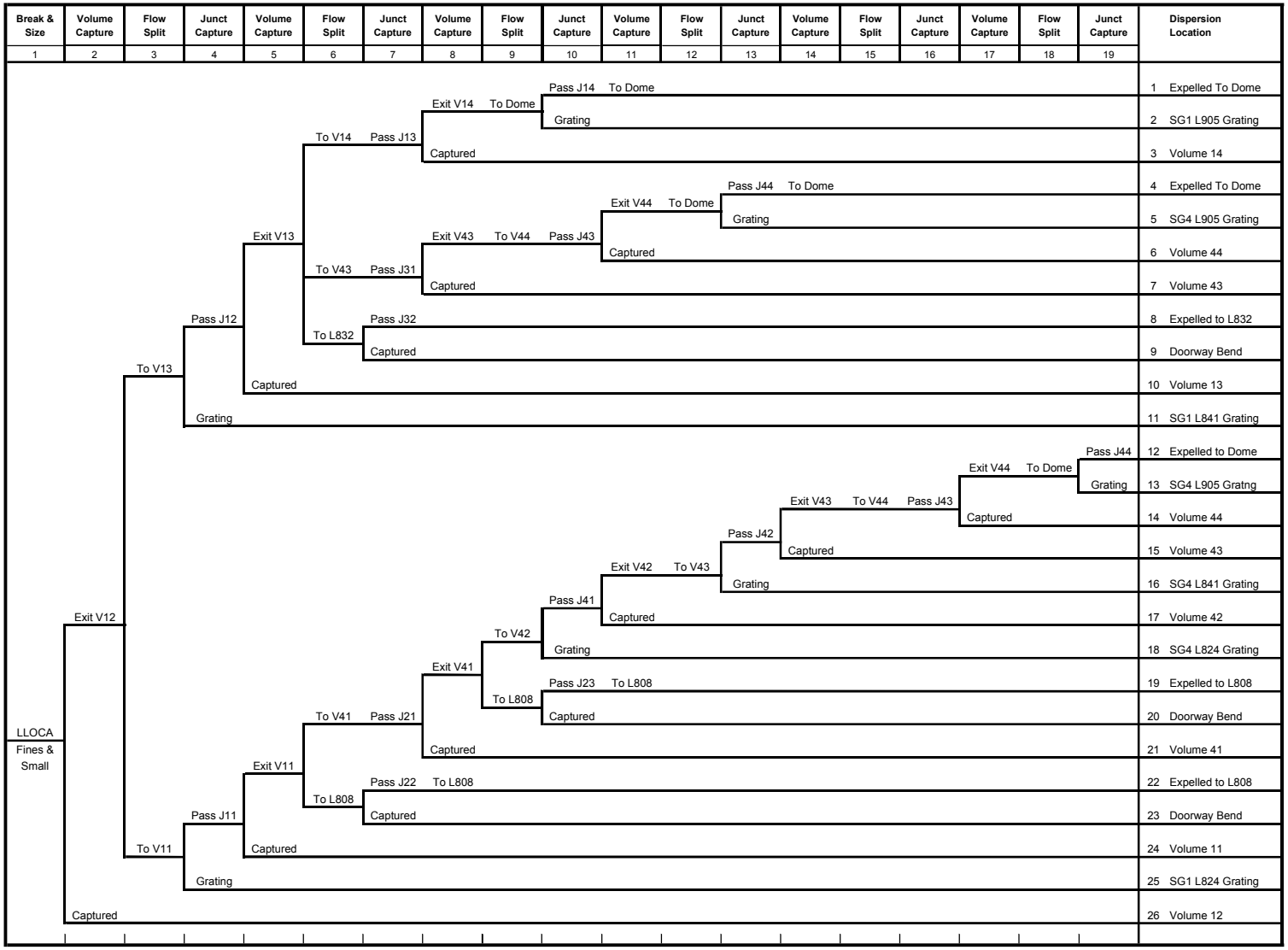

Figure VI-7. Chart for the Structure of Break-Region Debris Transport

VI.3.3.2 Dispersion and Capture throughout the Containment

The debris dispersion model used to evaluate debris transport within the volunteer-plant containments estimated dispersion throughout the containment first by free volume and then by surface orientation within a volume region. The model based the dispersion distributions first on actual volumes and areas and then adjusted them using weighting factors that were based on engineering judgment.

VI.3.3.2.1 Dispersion by Region

As the containment pressurizes following a LOCA, break flows carrying debris would enter all free volume within the containment. Larger debris would tend to settle out of the break flows as the flow slowed down after leaving the break region. However, the fine and smaller debris more likely would remain entrained so that fine and small debris would be distributed more uniformly throughout the containment. Certainly, the distribution would not be completely uniform because of debris being captured along the way, which is the reason for the weighting factors.

First, the containment free volume was subdivided into volume regions. This subdivision was based on geometry (i.e., floor levels and walls) and on the location of CSs. Specifically, areas where the CSs would not likely entrain the deposited debris were separated from areas that were impacted by the sprays. Some areas that were not actually sprayed still could be washed by the drainage of spray water as the water worked its way down through the containment structures. Areas where debris could be deposited without subsequently being washed downward by the sprays and the spray drainage could reduce the estimated transport fractions.

The total free volume of the containment is the sum of the free volumes for all of the volume regions. The volunteer-plant containment free volume was subdivided into a total of 24 volume regions (J = 24) as

$$V_{cont} = \sum_{j=1}^{J} Vc_j \quad ,$$

where

V_{cont} = the total free volume of the containment,

Vc_j = the free volume in containment region *j*, and

J = the number of volume regions.

The following equations define the dispersion model,

$$V_{i,j} = F_{i,j}\ D_i\ V_{ZOI} \quad ,$$

where

$V_{i,j}$ = the volume of debris-type *i* located in region *j*,

$F_{i,j}$ = the fraction of debris-type *i* deposited in region *j* during blowdown,

D_i = the fraction of total debris-type *i*, and

V_{ZOI} = the total volume of insulation contained within the ZOI.

For fibrous debris, the numbering system is *i* = 1, 2, 3, and 4 for fines, small pieces, large pieces, and intact debris, respectively.

The volume dispersion distribution must add up to one, as

$$\sum_{j=1}^{J} F_{i,j} = 1 \text{ (for each } i\text{)} \quad .$$

The break region was designated as Region 1 (i.e., *j* = 1 and $F_{i,1} = F_{i,break}$), and Section VI.3.3.1 of this appendix provides the methodology for the break-region dispersion fraction. The remaining distribution fractions were estimated using the volume and engineering judgment weighted distribution

$$F'_{i,j(j\neq 1)} = (1 - F'_{i,break}) \frac{wc_{i,j}\, Vc_j}{\sum_{j=2}^{J} wc_{i,j}\, Vc_j} \quad ,$$

where

$wc_{i,j}$ = the weighting factor based on engineering judgment.

If all of the $wc_{i,j}$ were set to one, then the distribution would be simply a volume-weighted distribution.

For large and intact pieces, many of these weighting values $wc_{i,j}$ were set to zero to reflect the fact that large and intact debris likely would not transport into many of the lower level volume regions. It is anticipated that most of the large and intact debris would reside in the break-region volume, sump-pool volume, containment-dome volume, or refueling area.

The substantial quantities of debris transported into the dome subsequently would tend to either fall out of the atmosphere or be washed out by the CSs. About half of this debris would be deposited onto the Level 905 floors that are associated with the dome. However, the other half would fall below this level, thereby entering other volume regions. The volume distribution function $F'_{i,j}$ is modified to account for debris fallout between regions as

$$F_{i,j} = F'_{i,j} + T_j \; F'_{i,2} \quad ,$$

where

T_j = the fraction of debris (type independent) located in the dome that subsequently falls or washes to region *j*.

The values of T_j are based on the opening areas into regions below the dome (e.g., the cross-sectional area of the SG compartments divided by the total cross-sectional area of the containment provides the values for debris that is falling into an SG compartment). The value for a region receiving no debris from dome fallout would be zero. Note that the dome volume region was designated Region 2; therefore, the value for Region 2 (i.e., T_2) must be negative to remove debris from Region 2, as

$$T_2 = -\sum_{j=1}^{J} T_{j(j\neq 2)} \quad .$$

VI.3.3.2.2 Dispersion by Surface Orientation and Exposure

Once the debris was dispersed to a volume region, the analysis assumed it to have been deposited within that region. Some residual fine debris could remain airborne in regions that are not impacted by the sprays; however, the total quantity of this residual airborne debris was not expected to be significant.

The surface area within each volume region was subdivided into six subsections. These subsections reflect both the differing surface orientations and their exposure to moisture. The floors were separated from all of the other surfaces because the floors would receive the gravitationally settled debris and the other surfaces could be flooded partially by spray drainage. The spray water would not accumulate on the other surfaces, which include the walls, ceilings, and equipment.

The analysis considered three surface exposures or moisture conditions—surfaces wetted directly by the CSs, surfaces not directly sprayed but washed by spray drainage (most likely floor surfaces), and surfaces wetted only by steam condensation. Condensation would likely wet all surfaces. The surface exposure determined how likely the flow of water would subsequently transport debris that was deposited onto that particular surface.

The following three-dimensional array describes these areas:

$A_{j,k,l}$ = area for volume region *j*, orientation *k*, and exposure *l*.

All of the area within a particular volume region then would be

$$A_j = \sum_{k=1}^{2} \sum_{l=1}^{3} A_{j,k,l} \quad .$$

The numbering system is *k* = 1 and 2 for floor and other surfaces, respectively, and *l* = 1, 2, and 3, for condensate, spray, and drainage exposures, respectively.

The surface-area distribution fractions were estimated using the following area and engineering judgment weighted distribution:

$$f_{i,j,k,l} = \frac{w_{i,j,k,l}\ A_{j,k,l}}{\sum_{k=1}^{2}\sum_{l=1}^{3} w_{i,j,k,l}\ A_{j,k,l}} \quad ,$$

where

$f_{i,j,k,l}$ = the fraction of debris-type *i* deposited within volume region *j* that was deposited onto surface *k*, *l*, and

$w_{i,j,k,l}$ = the weighting factor based on engineering judgment for debris-type *i* deposited within volume region *j* that was deposited onto surface *k*, *l*.

An equivalent expression for $f_{i,j,k,l}$ is

$$f_{i,j,k,l} = \frac{w_{i,j,k,l}\ g_{j,k,l}}{\sum_{k=1}^{2}\sum_{l=1}^{3} w_{i,j,k,l}\ g_{j,k,l}} \quad ,$$

where

$$g_{j,k,l} = \frac{A_{j,k,l}}{A_j} \quad .$$

The fractions summed within a particular volume region and for a particular debris type must add up to one:

$$\sum_{k=1}^{2}\sum_{l=1}^{3} f_{i,j,k,l} = 1 \quad .$$

If all of the $w_{i,j,k,l}$ were set to one, then the distribution would be simply an area-weighted distribution. If all the $w_{i,j,k,l}$ were set to zero for *k* = 2 (other surfaces), then all of the debris would be deposited on the floor, as likely would be the case for the large and intact debris. It is anticipated that most of the large and intact debris would reside on the floors in the break-region volume, sump-pool volume, containment-dome volume, or refueling area. In the SG compartment, much of the large debris stopped on the underside of a grating could fall back down after the depressurization flows subsided.

The volume of debris on a particular surface is expressed by

$$V_{i,j,k,l} = f_{i,j,k,l}\ F_{i,j}\ D_i\ V_{ZOI} \quad .$$

VI.3.4 Washdown Debris Transport

Potential washdown by the CSs, the drainage of the spray water to the sump pool, and (to a lesser extent) the drainage of condensate would subsequently affect the debris that is deposited throughout the containment. Debris on surfaces that would be hit directly by CS would be much more likely to transport with the flow of water than would debris on a surface that is wetted merely by condensation. The transport of debris entrained in spray water drainage is less easy to characterize. If the drainage flows were substantial and rapidly moving, the debris likely would transport with the water. However, at some locations, the drainage flow could slow and be shallow enough for the debris to remain in place. As drainage water dropped from one level to another, as it would through the floor drains, the impact of the water on the next lower level could splatter sufficiently to transport debris beyond the main flow of the drainage, thereby essentially capturing the debris a second time. In addition, the flow of water could erode the debris further, generating more of the very fine debris. These considerations must be factored into the analysis. Figure VI-8 illustrates the washdown processes schematically.

The drainage of spray water from the location of the spray heads down to the sump pool was evaluated. This evaluation provided insights for the transport analysis, such as identifying areas that were not impacted by the CSs, the water drainage pathways, likely locations for drainage water to pool, and locations where drainage water plummets from one level to the next.

VI.3.4.1 Debris Erosion during Washdown

Experiments conducted in support of the DDTS analysis demonstrated that the flow of water could further erode insulation debris. The DDTS analysis was primarily concerned with LDFG debris that was deposited directly below the pipe break and therefore was inundated by the break overflow. Debris erosion in this case was substantial (i.e., approximately 9 percent/h at full flow). Debris erosion caused by the impact of the sprays and spray drainage flows was certainly possible but was found to be much less significant. The DDTS study concluded that the CSs caused less than 1 percent of the LDFG to erode. The analysis neglected debris erosion occurring because of condensation and condensate flow. Debris with its insulation still in its cover was not expected to erode further. For RMI debris, erosion was not a consideration. However, for a microporous insulation such as calcium silicate or Min-K, the washdown erosion has not been determined; it would be expected to be substantial and could potentially erode this type of debris completely into fine silt.

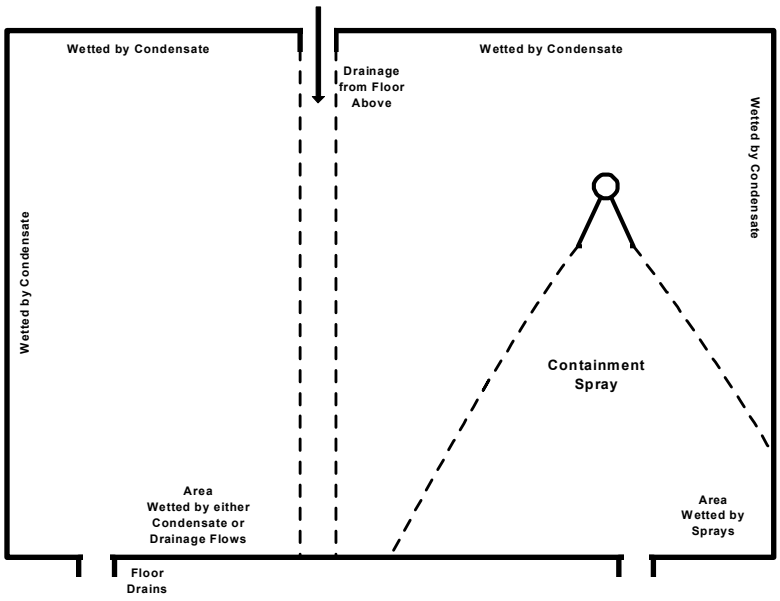

Figure VI-8. Schematic of Debris-Washdown Processes

Because the byproduct of the erosion process is more of the very fine and easily transportable debris, the process must be evaluated. All erosion products were assumed to transport to the sump pool. Because this debris would remain suspended in the sump pool until filtered from the flow at the sump screens, even a small amount of erosion could contribute significantly toward the likelihood of screen blockage.

The only erosion process evaluated herein was the erosion of debris that was impacted directly by the CSs. Erosion caused by break overflow was deferred to the degeneration of debris caused by sump pool turbulence associated with the plummeting of the break flow into the pool. This assumption neglects the erosion of any large debris that is deposited on top of the lower grating in SG1 and impacted directly by the break overflow; however, this quantity of debris was not considered to be substantial. Most of the debris that is located directly below the break likely would be pushed away from the break and into the sump pool. Note that the floors of the SG compartments are 4 ft above the floor of the sump pool. At switchover, the SG floor would not be flooded, but at the maximum pool height, that pool would have a depth of 0.7 ft in the SG compartment.

Table VI-4 summarizes the assumed fractions of fibrous debris that were eroded. It was assumed that condensate drainage would not cause further erosion of debris and that intact or covered debris would not erode further. Erosion does not apply to fine debris because that debris is already fine. About 1 percent of the small- and large-piece debris that the sprays directly impacted was considered to have eroded. This amount of erosion was considered to be conservative because the DDTS concluded that the erosion was less than 1 percent. No erosion of the intact debris was assumed because the canvas cover likely would protect the insulation.

Table VI-4. Total Erosion Fractions for Fibrous Debris

Exposure	Fines	Small	Large	Intact
Condensate	N/A	0	0	0
Sprays	N/A	1%	1%	0

To estimate the volume of debris that was eroded, the volume of debris that was impacted by the sprays first must be estimated. The latter estimate can be made using the data arrays that were already established in this methodology. These volumes for small and large debris, respectively, are estimated using the following two equations:

$$Vspr_2 = \sum_{j=1}^{J} \sum_{k=1}^{2} f_{2,j,k,2} \; F_{2,j} \; D_2 \; V_{ZOI}$$

and

$$Vspr_3 = \sum_{j=1}^{J} \sum_{k=1}^{2} f_{3,j,k,2} \; F_{3,j} \; D_3 \; V_{ZOI} \quad .$$

The volumes that are eroded (E_2 and E_3 for small and large debris, respectively) are simply 1 percent of the debris volumes impacted by the sprays, given as

$$E_2 = e_{spr} Vspr_2$$

and

$$E_3 = e_{spr} Vspr_3 \quad ,$$

where the spray erosion fraction e_{spr} is 0.01.

VI.3.4.2 Capture Retention during Washdown

The retention of debris during washdown must be estimated for the debris deposited on each surface (i.e., the fraction of debris that remains on each surface). The study assigned these estimates, based on experimental data and engineering judgment, somewhat generically. For surfaces that would be washed only by condensate drainage, nearly all deposited fine and small debris likely would remain there. The DDTS assumed that only 1 percent of the fibrous debris would be washed away in the more realistic central estimate of that study (a value of 10 percent was assumed for the upper bound estimate). When the analysis applied the 1 percent assumption, all of the surfaces that drained only condensate would have a retention fraction of 0.99 with respect to fibrous debris.

For surfaces that were hit directly by sprays, the DDTS assumed 50 percent and 100 percent for the central and upper bound estimates for small fibrous debris. Large and intact debris likely would not be washed down to the sump pool (retention fractions of 1).

For surfaces that were not sprayed directly but subsequently drain accumulated spray water, such as floors close to spray areas, the retention fractions were much less clear. These fractions likely would vary with location and drainage flow rates and therefore must be area location specific, with more retention for small pieces than for fine debris.

The retention fraction for a specific volume region is expressed as

$$R_{i,j} = \sum_{k=1}^{2} \sum_{l=1}^{3} f_{i,j,k,l} \; r_{i,j,k,l} \quad ,$$

where

$R_{i,j}$ = the fraction of debris-type *i* retained in region *j*, and

$r_{i,j,k,l}$ = the fraction of debris-type *i* retained, on surface *k*, *l*, in region *j*.

These volume region retention fractions $R_{i,j}$ do not account for the quantities that are eroded from the captured pieces of debris. To complete the erosion model, the analysis estimated the volumes of eroded debris that came from debris that remained captured versus debris that transported to the sump pool. Therefore, the debris that remained captured during the washdown process is estimated using the following two equations for small- and large-piece debris, respectively:

$$Rspr_2 = \sum_{j=1}^{J} \sum_{k=1}^{2} r_{2,j,k,2} \; f_{2,j,k,2} \; F_{2,j} \; D_2 \; V_{ZOI}$$

and

$$Rspr_3 = \sum_{j=1}^{J} \sum_{k=1}^{2} r_{3,j,k,2} \; f_{3,j,k,2} \; F_{3,j} \; D_3 \; V_{ZOI} \quad .$$

Therefore, the volumes of eroded debris associated with the debris that remained captured are expressed as

$$ER_2 = e_{spr} Rspr_2$$

and

$$ER_3 = e_{spr} Rspr_3 \quad .$$

Debris transported from its original volume region still could be captured at a lower elevation. This analysis neglected this secondary capture.

VI.3.5 Debris Volumes Introduced to the Sump Pool

The blowdown/washdown transport analysis primarily results in the volume that is transported to the sump pool by debris category. The volumes of debris transported to the pool are given by

$$V_{i,pool} = \left[1 - \sum_{j=1}^{J} R_{i,j} F_{i,j}\right] D_i \, V_{ZOI} + Ve_i \quad ,$$

where

$V_{i,pool}$ = the volume of debris-type *i* transported to the sump pool, and

Ve_i = the volumes of eroded debris transferring from small- and large-debris categories to the fine-debris category.

The erosion translation array is given by

$$Ve_i = \begin{bmatrix} +(E_2 + E_3) \\ -(E_2 - ER_2) \\ -(E_3 - ER_3) \\ 0 \end{bmatrix} \quad .$$

This array adds the eroded product ($E_2 + E_3$) to the fine-debris category and subtracts the eroded volume from the noncaptured small- and large-debris categories ($E_i - ER_i$). The total debris that transports to the pool is

$$V_{pool} = \sum_{i=1}^{4} V_{i,pool} \quad .$$

This model does not track debris transport in sufficient detail to determine where the debris would enter the sump pool. It assumed simply that the debris would mix uniformly with flows entering the pool.

VI.3.6 Transport Fractions

The overall debris-transport fraction now can be estimated as

$$TF_{ZOI} = \frac{V_{pool}}{V_{ZOI}} \quad ,$$

where

TF_{ZOI} = the fraction of insulation that is located in the ZOI and subsequently is transported to the sump pool.

The transport fractions for each individual debris category can be estimated as

$$TF_i = \frac{V_{i,pool}}{D_i \, V_{ZOI}} \quad ,$$

where

TF_i = the fraction of debris-type *i* that is generated within the ZOI and subsequently is transported to the sump pool.

Note that the transport fractions incorporate the translation of erosion products from the small- and large-debris categories to the fine-debris category.

VI.4 Debris-Transport Analysis

When the methodology presented in Section VI.3 was used, plausible estimates were developed for the transport of insulation debris within the volunteer-plant containments. Because of the complexity of the analysis and the limited available data, substantial uncertainty exists in these estimates. Engineering judgment that was used to fill gaps in the data was tempered conservatively. Despite the uncertainty, the transport analysis illustrated trends, as well as plausible estimates of the fractions of the debris that was generated and subsequently could transport to the sump pool.

VI.4.1 Fibrous Insulation Debris Transport

As discussed in Section VI.3.2, the insulation that is used in the volunteer-plant containments consists of fibrous, RMI, and Min-K insulation at approximately 13.4 percent, 85.7 percent, and 0.9 percent, respectively. The majority of the available debris-transport data was obtained for LDFG insulation debris, specifically experimental data taken for the DDTS (NUREG/CR-6369-2, 1999). Although a majority of the insulation within these containments is RMI, the fibrous insulation debris, in combination with particulate, is expected to be a larger challenge to the operation of the recirculation sump screens. Therefore, the debris transport for the fibrous debris was analyzed first. Even with the available transport data for LDFG debris, the transport analysis required the application of conservatively tempered engineering judgment.

VI.4.1.1 Fibrous Blowdown Debris Transport

The first consideration in performing the dispersion estimate for the fibrous blowdown insulation debris was the dispersion and deposition within the break region (assumed to be a break in SG1), where deposition likely resulted from inertial impaction. The dispersion through the remainder of the containment was subsequently estimated.

VI.4.1.1.1 Break-Region Blowdown Debris Deposition

The effluences from the break would carry insulation debris with the flows into the upper containment dome through the large opening at the top of the SG compartment and into lower compartments through the compartment access doorways. Along the way, substantial portions of that debris likely would be inertially deposited or otherwise

entrapped onto structures. In general, the break-region flow immediately after the initiation of the break would be much too violent to allow debris simply to settle to the floor of the region.

VI.4.1.1.1.1 Characterize Break Flows within Break Region

The thermal-hydraulic MELCOR code was used to determine the distribution of the break effluents from the SG compartment. When a break in SG1 was postulated, it was determined that most of the break effluent would be directed upward toward the large upper dome. Because of the large openings connecting SG1 to SG4, the venting to the dome would occur through both SG compartments. Effluents venting into lower level compartments (surrounding the two SGs) by way of open access doorways would flow at much lower rates than the upward flows to the dome. Figure VI-6 shows the nodalization of the two SG compartments, where the break was postulated to occur in Volume V12. The analysis assumed break effluents that are typical of three break sizes—large-break (LB) LOCA, medium-break (MB) LOCA, and small-break (SB) LOCA. Table VI-5 summarizes the results of the MELCOR simulations and shows the distributions from a particular control volume by the connecting junction. For example, given an LBLOCA scenario, approximately 80 percent of the flow from Volume V12, where the break was postulated, went upward through Junction J12, with the remainder going downward through Junction J11. Note that the flow splits were somewhat transient and that the results in Table VI-5 are reasonable approximations of the transients over the time where most debris transport would occur. The LBLOCA and MBLOCA flows were reasonably steady over the transport period, but SBLOCA flows were not steady because of transition into natural circulation after approximately 6 s.

Inertial debris deposition depends on the flow velocities transporting the debris. The MELCOR calculations predicted transient flow velocities for each flow junction and each size of break. Table VI-6 provides the general ranges of these velocities. The velocities are in the general range as the test velocities for which the DDTS measured the debris-capture data.

Table VI-5. Break Effluent Flow Splits

Break Size	Flows Exiting Volume V_i through Junction J_j								
	V12		V11		V41		V13		
	J11	J12	J21	J22	J23	J41	J13	J31	J32
LBLOCA	20%	80%	70%	30%	5%	95%	62%	33%	5%
MBLOCA	20%	80%	70%	30%	14%	86%	62%	33%	5%
SBLOCA	15%	85%	80%	20%	30%	70%	66%	28%	6%

Table VI-6. Characteristic Velocities in SG1

Postulated Break Size	Characteristic Velocities	
	m/s	ft/s
LBLOCA	25–200	80–660
MBLOCA	5–45	15–150
SBLOCA	1–8	5–25

VI.4.1.1.1.2 Debris-Transport Distributions from Volumes

The very fine debris would transport more like an aerosol in that the particles would disperse within the flow and follow the flow. Portions of this debris would be deposited onto structures along the transport pathways, primarily because of inertial deposition at bends in the flow. However, with larger debris, the tendency would be greater for the debris not to follow the flow through sharp bends in the flow and larger debris would more likely be trapped by a structure such as a grating. In addition, gravitational settling as the flow velocities slow would be more effective for larger debris than smaller debris. For example, following an LBLOCA in an SG compartment, a large, nearly intact insulation pillow could travel upward with the main flow to the containment dome unless an obstacle, such as a grating, impeded that pillow. However, this pillow would be much less likely to follow the flow through a connecting doorway to the next SG compartment.

The solution to this problem required assumptions based on engineering judgments that were tempered by experimental observations. The assumptions provide a reasonable crude approximation of debris transport from a volume when there is a split in the flow. These assumptions include the following:

- The fine and small fibrous debris would be well dispersed within the flow and would transport uniformly with the flow; therefore, the debris-transport junction distributions for fines and small debris are the same as the junction flow distributions in Table VI-7.
- Large and intact debris would not make the turn to exit SG1 at Level 832 (Junctions J31 and J32). In addition to the turn, the gratings that cover approximately 45 percent of the cross-sectional area of the compartment that is nearest those exits would stop most of this debris that was moving towards these exits.
- Large and intact debris entering SG4 at the floor level (Level 812) would be much less likely to follow the flow through the 90-degree bend and subsequently transport upward through SG4. Debris entering Volume V41 that is not captured in Volume V41 would exit by either Junction V23 or V41. For large and intact debris, the flow fractions for Junction V41 were reduced by one-half and two-thirds, respectively, based on engineering judgment.

Applying these assumptions to the transport of the large and intact debris through the node junctions resulted in the junction transport distributions that are shown in Table VI-7 and Table VI-8.

Table VI-7. Large-Debris-Transport Junction Distributions

Break	V12		V11		V41		V13		
	J11	J12	J21	J22	J23	J41	J13	J31	J32
LBLOCA	20%	80%	70%	30%	52%	48%	100%	0%	0%
MBLOCA	20%	80%	70%	30%	57%	43%	100%	0%	0%
SBLOCA	15%	85%	80%	20%	65%	35%	100%	0%	0%

Table VI-8. Intact-Debris-Transport Junction Distributions

Break	V12		V11		V41		V13		
	J11	J12	J21	J22	J23	J41	J13	J31	J32
LBLOCA	20%	80%	70%	30%	68%	32%	100%	0%	0%
MBLOCA	20%	80%	70%	30%	71%	29%	100%	0%	0%
SBLOCA	15%	85%	80%	20%	77%	23%	100%	0%	0%

VI.4.1.1.1.3 Capture Fractions at Junctions

Debris-transport data from the Army Research Laboratory (ARL) and the CEESI tests that were conducted to support the DDTS (NUREG/CR-6369-2, 1999) provide average capture fractions for LDFG debris that is passing though typical gratings and around typical structures, such as piping and beams, and for debris making a 90-degree bend. These structures and the bend were wetted during the tests; the data do not apply to dry structures. These data are assumed to apply in general to the volunteer-plant containments because it is expected that steam condensation,* as well as liquid break effluent, would rapidly wet the containment surface and because the range of predicted flow velocities (Table VI-6) are in general agreement with the flow velocities of the tests. The flow velocities ranged from 25 to 150 ft/s for the ARL tests and from 35 to 60 ft/s for the CEESI tests. The debris capture applied most to MBLOCAs and perhaps least to SBLOCAs.

Fine and small fibrous debris could be captured inertially onto wetted surfaces whenever the break flow changed direction, such as flows through the doorways from the SG compartments into the sump-level annular space. These flows must make at least one 90-degree bend through those entrances. Debris-transport experiments that were conducted at CEESI demonstrated an average capture fraction of 17 percent for fine and small debris that were making a 90-degree bend. These surfaces would be wetted because of steam condensation and the liquid portion of the break effluence. Other flow bends likely would occur within the violent three-dimensional flows near the break. The platform gratings within the SG compartments would capture substantial amounts of debris, even though the gratings do not extend across the entire compartment. The CEESI debris-transport tests demonstrated that an average of 28 percent of the fine and small LDFG debris was captured when the airflow passed through the first wetted grating encountered and that an average of 24 percent was captured at the second grating. A grating would completely trap the large and intact debris. In addition, the tests showed equipment (such as beams and pipes) to capture fine and small debris. In

* Based on analyses performed for the DDTS (NUREG/CR-6369-3, 1999).

the CEESI tests, the structural maze in the test section captured an average of 9 percent of the debris passing through the maze.

In the volunteer plant, partial gratings exist at three levels in each of the SG compartments. The gratings extend over approximately 22 percent, 45 percent, and 15 percent of the SG cross-sectional area at plant elevations 824, 841, and 905 ft, respectively.* If it is assumed that a grating captures 28 percent of small and fine fibrous debris and 100 percent of the large and intact debris from the flow as it passes through the grating, Table VI-9 provides the capture fractions for model junctions that contain a grating.

Table VI-9. Grating Capture Fractions at Model Junctions

Grating Level	Model Junctions	Fine and Small Debris		Large and Intact Debris	
		Unit Area Capture Fraction	Junction Capture Fraction	Unit Area Capture Fraction	Junction Capture Fraction
Level 905	J14 and J44	0.28	0.04	1.0	0.15
Level 841	J12 and J42	0.28	0.13	1.0	0.45
Level 824	J11 and J 41	0.28	0.06	1.0	0.22

Depressurization flows also would exit the SGs by way of the SG access doorways at Levels 808 and 832. Flows traveling through these pathways would carry debris directly into the lower levels of the containment; in fact, some of the debris likely would be deposited near the recirculation sumps. Because these doorways were designed with at least one 90-degree bend, debris would be deposited inertially onto wetted surfaces at each bend in the flow. Furthermore, because the CSs would not impact these vertical surfaces, the debris likely would remain on the surfaces once it was captured there. The CEESI data showed an average of 17 percent debris capture at its 90-degree bend for debris that was small enough to already have passed through a grating (i.e., fines and small debris). The analysis assumed that 17 percent of fine and small debris that was transported from the SG break region through the Level 808 and Level 832 doorways to the bulk containment would be captured at a bend (one bend assumed). No comparable data exist for the large and intact debris; however, the larger debris would be much less likely to stick to a wall once it impacted inertially against the wall. Because of a lack of appropriate data, it was assumed conservatively that these doorways would capture no large or intact debris.

VI.4.1.1.1.4 Capture Fractions within Volumes

As illustrated in Table VI-9, debris would be captured on structures within the model nodes, as well as the node junctions. As the break effluents flowed around and through the structural and equipment congestion within the SG compartment, debris would be

*These fractions were estimated from plant drawings.

driven inertially onto surfaces where some portion of it would remain captured. The structures include the pumps, SGs, and associated piping, beams, equipment stands, cabling, and other items. The chaotic nature of the flows as the break jet is deflected off structures and wall surfaces could create a multitude of bends in the flow that could deposit debris inertially onto wall surfaces and irregular wall features. In the CEESI tests, approximately 9 percent of the fine and small debris was deposited onto wetted structures as the debris passed through a test structural assembly and 17 percent was captured onto a wetted surface at a sharp 90-degree bend in flow. Estimates of the amounts of debris captured within a node volume were based on this CEESI test data and on conservatively tempered engineering judgment. It is likely conservative to capture more debris within the SG than to transport the debris throughout the containment because washdown within the SG should be relatively greater than some other areas of the containment and because debris washed off the SG structures can go directly to the sump pool.

Applying a number of engineering judgments in conjunction with the CEESI data resulted in estimates for the capture of debris within each volume of the break-region debris-transport model. Table VI-10 provides these estimates, along with the associated assumptions.

Table VI-10. Fractions of Debris Captured within Each Volume

SG1				SG4			
Volume	Fines and Small Pieces	Large Pieces	Intact Pieces	Volume	Fines and Small Pieces	Large Pieces	Intact Pieces
V14	1% (A)	2% (A)	5% (A)	V44	1% (A)	2% (A)	5% (A)
V13	1% (A)	2% (A)	5% (A)	V43	1% (A)	2% (A)	5% (A)
V12	14% (C)	30% (E)	50% (F)	V42	9% (B)	15% (E)	30% (G)
V11	26% (D)	40% (E)	80% (H)	V41	14% (C)	25% (E)	80% (H)

Assumptions
A. Volumes contain minimal structures and no significant flow bends; therefore, a minimal amount of capture occurs. It is somewhat more likely that large debris would be captured than small debris and more likely that intact debris would be captured than large debris.
B. Structures are equivalent to one CEESI structural test assembly (9 percent), and no significant flow bends exist.
C. Structures are equivalent to one CEESI structural test assembly (9 percent), and significant flow bending that is less than a sharp 90-degree bend exists (5 percent).
D. Structures are equivalent to one CEESI structural test assembly (9 percent), and significant flow bending that is equivalent to a sharp 90-degree bend exists (17 percent).
E. Large debris is more likely to be captured than small debris, and 50 percent more large debris is captured than small debris.
F. Intact debris is much more likely to snag on equipment than the large debris. In addition, some insulation within the ZOI likely could remain attached to piping.
G. Intact debris is much more likely to snag on equipment than the large debris.
H. The congestion of equipment and cables near the floor is expected to trap most of the intact debris as the flow makes a 90-degree bend near the floor. Intact debris is less likely to follow the distribution of flow than is smaller debris.

VI.4.1.1.1.5 Break-Region Debris-Transport Quantification

The logic chart shown in Figure VI-7 and discussed in Section VI.3.3.1 was used to quantify the various flow splits and capture and to estimate the debris deposition within and from SG1. The chart divides the evaluation into many smaller problems that are amenable to resolution—an approach that was adapted from the resolution of the BWR strainer-blockage issue (NUREG/CR-6369-1, 1999). This chart tracks the progress either of small debris from the pipe break (Volume V12) until the debris is assumed to be captured or until the debris is transported beyond the compartment. Charts were quantified for each of the three LOCA sizes (i.e., small, medium, and large) and for three classifications of fibrous debris (i.e., fines and small pieces, large pieces, and intact pieces). Note that there was no basis to treat the fines and small pieces differently. Sections VI.4.1.1.1.1 through VI.4.1.1.1.4 discuss the data that were used to quantify the charts. As an example, Figure VI-9 shows the chart for the transport of fines and small debris following an LBLOCA.

Table VI-11 shows the overall results of the break-region quantification. The results for the three break sizes were averaged into a single set of results because the differences among the three size groups were substantially less than the substantial uncertainties associated with these analyses. The charts also provided information regarding the distribution of debris captured with the SGs, as well as the debris driven from the SGs.

Table VI-11. Distribution of Debris Captured and Exiting Break Region

Location	Debris Category		
	Fines and Small Pieces	Large Pieces	Intact Pieces
Captured within SGs 1 and 4	0.36	0.70	0.82
Expelled to Dome	0.58	0.26	0.17
Expelled to Level 832	0.03	0	0
Expelled to Level 808	0.03	0.04	0.01

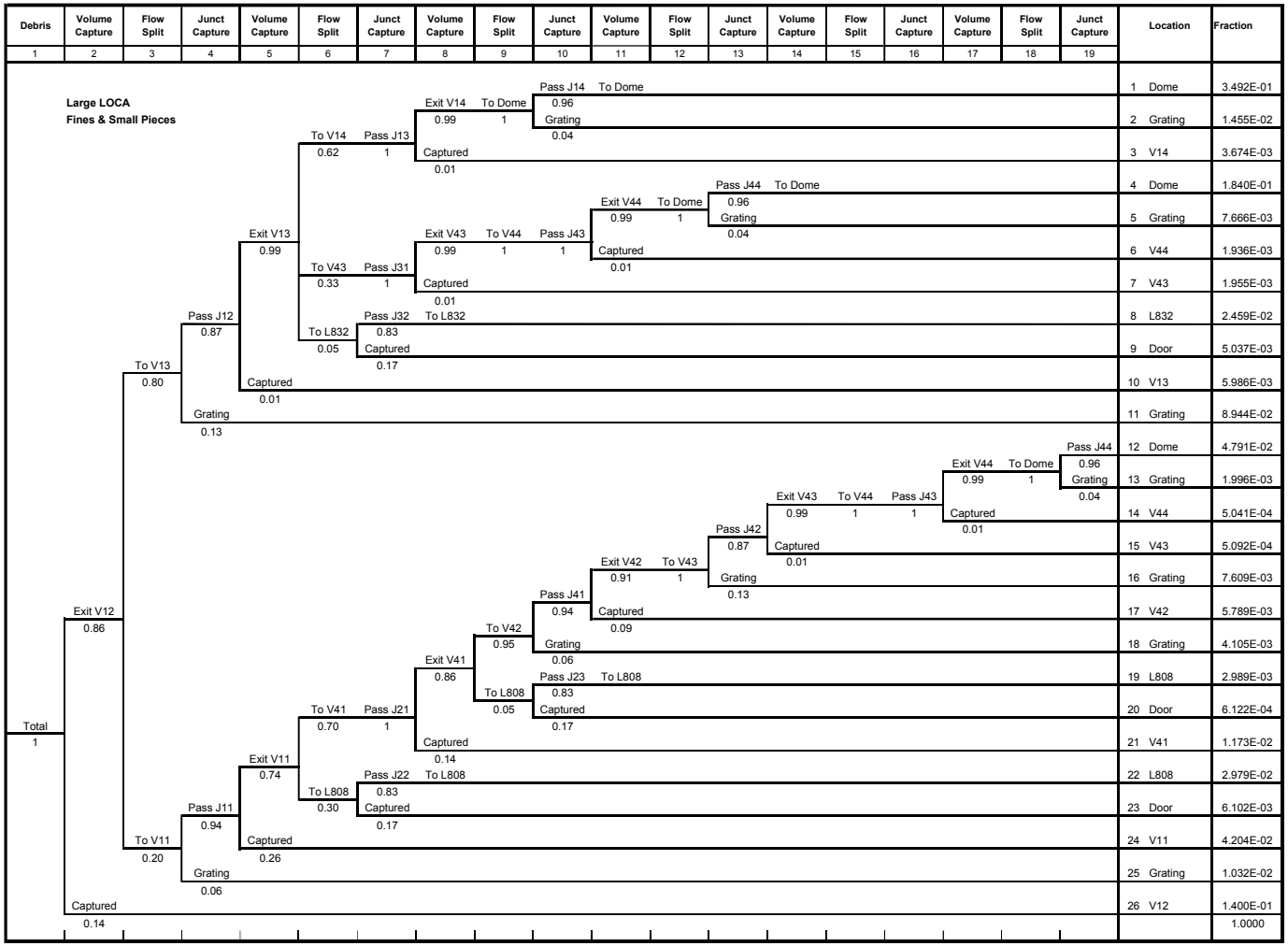

Figure VI-9. Break-Region LBLOCA Transport Chart for Fines and Small Debris

VI.4.1.1.2 Dispersion throughout Remainder of Containment

Section VI.3.3.2 presents the debris dispersion model used to evaluate debris transport within the volunteer-plant containments by estimating dispersion throughout the containment first by free volume and then by surface orientation within a volume region.

VI.4.1.1.2.1 Dispersion by Volume Region

The containment free volume was subdivided into volume regions that were based on geometry, such as floor levels and walls, and on the location of CSs. Specifically, areas where CSs would not likely wash down deposited debris were separated from areas that were impacted by the sprays. The volunteer-plant free volume was subdivided into 24 distinct regions, as shown in Table VI-12. The volumes of each region were estimated from plant drawings.

Table VI-12. Subdivision of Containment Free Volume

No.	Volume Region	Volume (ft^3)	Volume Fraction Vc_j
1	SG1&4	76600	0.02570
2	Dome—Above 905.75-ft	1992060	0.66848
3	L873—MS	39300	0.01319
4	Head Lay-Down—L871.5	17120	0.00574
5	Below Head Platform	5750	0.00193
6	Refueling A	45340	0.01521
7	Refueling B	53860	0.01807
8	Refueling C	48660	0.01633
9	Refueling D	47960	0.01609
10	SG2&3	76600	0.02570
11	Pressurizer	11250	0.00378
12	L860 Annulus—Section 1	34100	0.01144
13	L860 Annulus—Section 2	54580	0.01832
14	L860 Annulus—Section 3	94310	0.03165
15	L851—FW	25800	0.00866
16	Accumulator Section	31500	0.01057
17	L832 Annulus—Section 1	37250	0.01250
18	L832 Annulus—Section 2	33940	0.01139
19	L832 Annulus—Section 3	69890	0.02345
20	L808 Annulus—Section 1	61650	0.02069
21	L808 Annulus—Section 2	30830	0.01035
22	L808 Annulus—Section 3	61650	0.02069
23	Reactor Cavity	25000	0.00839
24	Equipment Room L808	5000	0.00168
	Containment Total	2980000	1.00000

Key aspects of the region subdivision follow. The first region, designated SG1 and 4, is the SG compartment 1 where the break was postulated and its connected neighboring SG compartment, SG4. Section VI.4.1.1.1 predicted debris dispersion and deposition in

these SG compartments. The second region represents the free volume above the highest floor (i.e., the dome region), which is approximately two-thirds of the entire containment free volume. As shown in Figure VI-10, the lower floor levels were subdivided azimuthally into three sectors to better distinguish the areas with CSs from areas without the sprays. The refueling pool area was subdivided into four regions to reflect the three different pools and the reactor vessel head area (i.e., (A) storage pool for reactor vessel upper internals, (B) reactor vessel area, (C) storage pool for reactor vessel lower internals, and (D) pool for fuel transfer and storage).

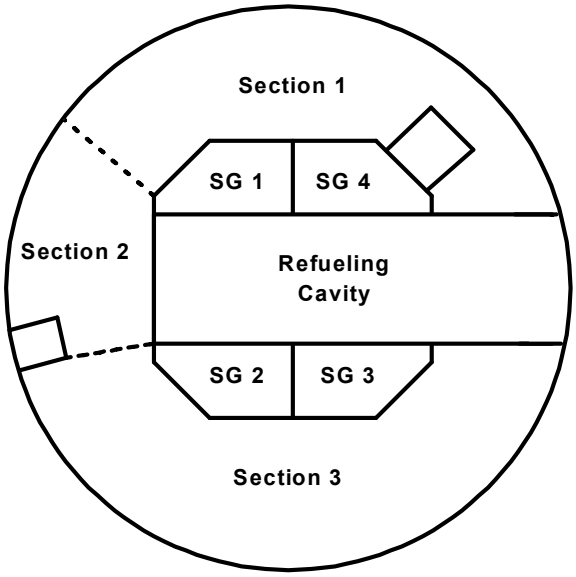

Figure VI-10. Volume Region Sector Model

Debris, particularly the larger debris, would not distribute uniformly throughout the free volume. The methodology presented in Section VI.3.3.2.1 applies weighting factors ($wc_{i,j}$) to the free-volume distribution to estimate the distribution of debris throughout the containment (i.e., the distribution of the debris among the 24 volume regions) by debris type. The very fine debris likely would transport somewhat uniformly with the depressurization flows, which would penetrate all free space within the containment as the containment pressurized. The transient nature of debris generation would also introduce nonuniformities into the dispersion of the fine debris. Because no rationale was found to weight the distribution of the fine and small debris away from that of a uniform free-volume distribution outside the break region, all weighting factors were assumed to be 1 for fine and small fibrous debris.

For the largest debris, specifically the large-piece and intact-piece classifications, the debris that is ejected from the SG compartments into the dome region likely would fall back to the floors and structures of the higher levels. The settling of debris that was ejected into the dome atmosphere was proportioned onto the upper floors according to the distribution of floor area (e.g., the cross-sectional area of a SG compartment divided by the cross-sectional area of the overall containment determined the fraction of settling debris that would fall into that compartment). The largest debris likely would not enter lower compartment volumes, except for debris ejected into the sump-level annulus via

personnel access doorways. The assumed weighting factors for the large and intact debris were specified to give preference to the deposition of larger debris onto the uppermost floors and into the sump-level annulus. The large-piece debris was assumed to transport somewhat more easily than the intact-piece debris. Table VI-13 shows the assumed weighting factors and the dome fallout fractions.

Table VI-13. Volume Region Weighting Factors

No.	Volume Region	Dome Fallout Fraction T_j	Volume Weighting Factors			
			Fines $wc_{1,j}$	Small Pieces $wc_{2,j}$	Large Pieces $wc_{3,j}$	Intact Pieces $wc_{4,j}$
1	SG1&4	0.0951	1	1	1	1
2	Dome - Above 905.75-ft	0	1	1	1	1
3	L873 - MS	0.0555	1	1	0.5	0.3
4	Head Lay-Down - L871.5	0.0349	1	1	0.8	0.5
5	Below Head Platform	0	1	1	0.3	0
6	Refueling A	0.0495	1	1	0.8	0.5
7	Refueling B	0.0579	1	1	0.8	0.5
8	Refueling C	0.0505	1	1	0.8	0.5
9	Refueling D	0.0596	1	1	0.8	0.5
10	SG2&3	0.0978	1	1	0.5	0.3
11	Pressurizer	0	1	1	0	0
12	L860 Annulus - Section 1	0.0092	1	1	0.3	0
13	L860 Annulus - Section 2	0.0052	1	1	0.3	0
14	L860 Annulus - Section 3	0.0241	1	1	0.3	0
15	L851 - FW	0	1	1	0	0
16	Accumulator Section	0.0060	1	1	0.8	0.5
17	L832 Annulus - Section 1	0	1	1	0	0
18	L832 Annulus - Section 2	0	1	1	0	0
19	L832 Annulus - Section 3	0	1	1	0	0
20	L808 Annulus - Section 1	0	1	1	1	1
21	L808 Annulus - Section 2	0	1	1	1	1
22	L808 Annulus - Section 3	0	1	1	0.3	0
23	Reactor Cavity	0	1	1	0	0
24	Equipment Room L808	0	1	1	0	0
	Total	0.5453				

Figure VI-11 illustrates the results of the blowdown distribution by groups of volume regions. In this estimate, the largest portion of the debris was deposited inside the SG compartments, where the break was postulated, because of inertial deposition that occurred as the fast-moving flows drove the debris into and through equipment and structures. This was particularly true for the larger debris, which could not pass through the gratings. The upper level floors (871-, 873-, and 905-ft levels) received substantial debris falling or settling out of the dome atmosphere. The regions above the refueling pools received debris that was driven into those volumes, as well as debris falling or settling from the dome atmosphere; this comment also applies to the opposite SG

compartments, SGs 2 and 3. The pressurizer compartment received only small amounts of fine and small debris and no larger debris because the compartment has a roof that prevents debris from falling into the compartment and is relatively small. The lower levels received relatively small quantities of mostly large-piece debris because of their remoteness from the dome. Most of the debris entering Levels 832 and 808 was debris that was expelled from the SG compartments by way of the personnel access doorways; therefore, this debris would likely be located near those doors.

The CSs would impact most of the deposited debris; these surface areas include the four SG compartments, the upper floor surfaces, and the refueling area. The sprays did not impact regions such as the pressurizer compartment and certain portions of the lower levels. This observation suggests that a large fraction of the more transportable debris would move to the sump pool.

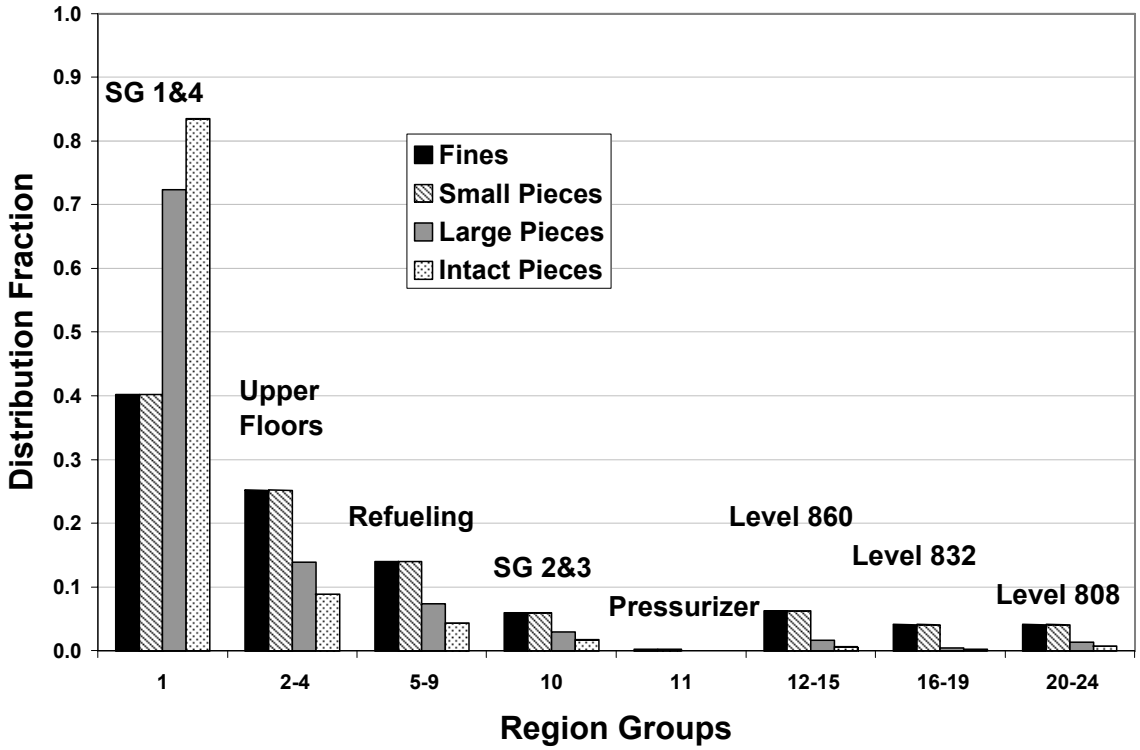

Figure VI-11. Blowdown Distribution by Region Groups

VI.4.1.1.2.2 Dispersion by Surface Orientation and Surface Wetness

Once the debris dispersion prediction placed each type of debris within the 24 volume regions, the debris was dispersed further by surface area classification (i.e., orientation and exposure to moisture). The surface orientation was either floor area or other area, distinguished by the fact that gravitational settling preferentially deposited debris onto the floor. The surface exposure to moisture included surfaces that the CSs impacted directly, surfaces subjected to spray drainage but not sprayed directly, and the remaining surfaces, which would be wetted by condensation. In this manner, the surface area within each volume region was subdivided into six surface groupings. This subdivision

was based on both engineering drawings and engineering judgment. The drawings provided basic geometric information such as floor areas; however, engineering judgment, in addition to drawings, was required to estimate fractions of surfaces that were sprayed directly or covered by spray drainage. Table VI-14 shows the estimated area distribution fractions.

The floor fraction is an estimate of the total surface area that would receive gravitationally settling debris. This estimate includes upward-facing equipment, as well as the floor (the equipment and piping was assumed to have the same floor fraction as the wall, floor, and ceiling surfaces). The condensate, spray, and drainage fractions represent the fraction of each orientation with this type of exposure. With these fractions, the surface areas and area ratios (i.e., $A_{j,k,l}$ and $g_{j,k,l}$) are determined. For example, the floor fraction for a given region multiplied by the spray $g_{j,k,l}$ fractions for that region's floor multiplied by the total surface area of the region yields the floor surface area that was sprayed directly by the sprays.

Table VI-14. Regional Areas Fractions

No.	Volume Region	Floor Fraction	Floor Surface Area			Other Surface Area		
			Condensate Fraction	Spray Fraction	Drainage Fraction	Condensate Fraction	Spray Fraction	Drainage Fraction
1	SG1&4	0.07	0	1	0	0.1	0.5	0.4
2	Dome - Above 905.75-ft	0.09	0	1	0	0	1	0
3	L873 - MS	0.17	0.2	0.6	0.2	0.9	0.1	0
4	Head Lay-Down - L871.5	0.61	0	1	0	0	0	1
5	Below Head Platform	0.30	0.6	0.1	0.3	0	0	1
6	Refueling A	0.37	0	1	0	0	0	1
7	Refueling B	0.41	0	1	0	0	0	1
8	Refueling C	0.55	0	1	0	0	0	1
9	Refueling D	0.68	0	1	0	0	0	1
10	SG2&3	0.07	0	1	0	0.1	0.5	0.4
11	Pressurizer	0.04	1	0	0	1	0	0
12	L860 Annulus - Section 1	0.10	0.9	0.1	0	1	0	0
13	L860 Annulus - Section 2	0.19	0.1	0.6	0.3	0.6	0.1	0.3
14	L860 Annulus - Section 3	0.19	0.1	0.6	0.3	0.6	0.1	0.3
15	L851 - FW	0.19	0.8	0	0.2	1	0	0
16	Accumulator Section	0.13	0	0.5	0.5	0.5	0	0.5
17	L832 Annulus - Section 1	0.18	0.9	0	0.1	0.7	0	0.3
18	L832 Annulus - Section 2	0.15	0.4	0	0.6	0.6	0	0.4
19	L832 Annulus - Section 3	0.17	0.3	0.5	0.2	0.6	0	0.4
20	L808 Annulus - Section 1	0.18	0	0	1	0.7	0.3	0
21	L808 Annulus - Section 2	0.18	0	0	1	0.7	0.3	0
22	L808 Annulus - Section 3	0.19	0	0	1	0.7	0.3	0
23	Reactor Cavity	0.13	0	0	1	1	0	0
24	Equipment Room L808	0.21	0	0	1	1	0	0

Next, the area weighting factors ($w_{i,j,k,l}$) were estimated, which preference debris toward one surface over another. The dominant preferential debris deposition (and the only preference that can be estimated realistically) is gravitational debris that settles to the floor surfaces. The weighting factors for the nonfloor surfaces ($k = 2$) were set first to 1 (i.e., $w_{i,j,2,l} = 1$), and then the weighting factors for the floor surfaces within each volume region were estimated for each debris type such that the weighting factors

preferentially forced debris deposition onto the floor surfaces. The floor weighting factor estimates used the following equation, where the weighting factor is a function of two physical variables that can be estimated more readily. These variables are the fraction of the surface area that is floor area (a geometric determination) and the fraction of the debris that is deposited onto the floor (an engineering judgment and computational determination):

$$w_{floor} = \left(\frac{d_{floor}}{1-d_{floor}}\right)\left(\frac{1-g_{floor}}{g_{floor}}\right) \quad ,$$

where

w_{floor} = the weighting factor for debris deposited onto the floor inside a volume,

d_{floor} = the fraction of the debris deposited within a volume that was on the floor, and

g_{floor} = the fraction of the volume surface area that is floor area.

The determination of the floor-area fraction (g_{floor}) is a straightforward estimate of the floor area divided by the total surface area in a volume region (listed in Table VI-14). In actuality, the surface-area estimate includes the areas associated with equipment and piping because debris can settle onto equipment and piping, as well as onto floors. To reduce the complexity of the area estimates, it was assumed that the area fractions for the equipment and piping were the same as the area fractions for the wall, ceiling, and floor surfaces. Because of this assumption and other geometrical assumptions, these area fractions have an inherent uncertainty associated with the estimates; however, this uncertainty should be significantly smaller than some of the other transport uncertainties.

Debris deposition processes other than gravitational settling, such as diffusiophoresis (condensation-driven deposition), do not depend on surface orientation for these processes; the weighting factors all would be set to 1. Driven debris could be deposited inertially onto any surface or could snag on an obstacle. Heavy, inertially deposited debris subsequently may fall to the floor, but substantially smaller debris likely would remain pasted onto the surface. Even heavy debris can remain on a nonhorizontal surface if the piece were physically snagged. Vertically moving debris eventually would settle onto a surface that is sufficiently horizontal to retain the debris. The fraction of debris deposition onto the floor is highly dependent on the size of the debris.

The estimate of the fraction of the debris that was deposited onto the floor depended greatly on conservative judgments; therefore, the fraction introduced substantial uncertainty into the transport estimates. The engineering judgments accounted for the geometry of the region under consideration, including the relative structural congestion. It was conservative to place the debris on the floor as opposed to other surfaces because more of the debris that was deposited on the floor would be subjected to spray washdown on the floor than on other surfaces. For the SG compartments where the pipe break was postulated (SGs 1 and 4), debris deposition data from the logic charts were used to estimate debris on the floor of these compartments. This estimate included larger debris that was trapped on the underside of gratings and that would likely fall back once the depressurization flow subsided. It was assumed that debris that fell or

settled from the dome atmosphere into lower level regions would fall or settle onto a floor surface.

A typical judgment estimate for fractions of debris that had been driven into an enclosure and that would subsequently settle to the floor was 0.4, 0.7, 0.99, and 0.99 of the fines, small pieces, large pieces, and intact pieces, respectively. For fine debris, the floor deposition fraction was two to three times the floor area fraction, thereby allowing a substantial settling of the very fine debris, even though diffusion processes would deposit the fine debris onto any surface. The floor fraction for small-piece debris was substantially higher than for the fine debris. Large and intact debris would fall to a horizontal surface unless it snagged on an obstacle. The floor fraction was set to 0.99 to place the large debris on the floor; however, some pieces could have snagged on an obstacle before reaching the floor.

For the far-side SG compartments (SGs 2 and 3) and the pressurizer compartment, the floor-debris deposition fractions acknowledged that the debris would have to travel downward in the compartment and through a variety of structures, including gratings, before reaching the floor; the fractions were reduced for these compartments. For instance, the gratings would catch much of the large debris before it could reach the floor. For open regions, such as the refueling pool regions, where a small amount of equipment and piping is located and the region is not enclosed completely by walls, the floor-debris fractions were increased substantially.

Once the weighting factors were estimated, the final deposition of the debris was determined both as a function of the region and by the surface orientation and its exposure to moisture. Figure VI-12 and Figure VI-13 illustrate the dispersion patterns in the containment according to surface orientation and surface wetness.

In Figure VI-12, all of the LOCA-generated debris is distributed fractionally according to surface orientation (floor surfaces or other surfaces), whether the debris was captured within the break region (SGs 1 and 4), and debris type. This distribution reflects the debris-generation size distribution of Table VI-2 and the break-region capture fractions of Table VI-11. For the fines and small-piece debris, the largest fractions corresponded to floor surfaces outside or beyond the break region; debris preferentially settled onto the floors. Most of the debris that was captured within the break region was located on other structures that correspond to equipment, piping, and gratings within those SG compartments. For the larger debris, the congestion of structures trapped the majority of the debris within the break region. Nearly half of this debris either was deposited onto the floor of the break region or was assumed to fall to the floor after the break flows subsided. Most large debris that was ejected from the break region was predicted to fall out onto floor surfaces; therefore, small amounts of large debris were found on other structures outside of the break region.

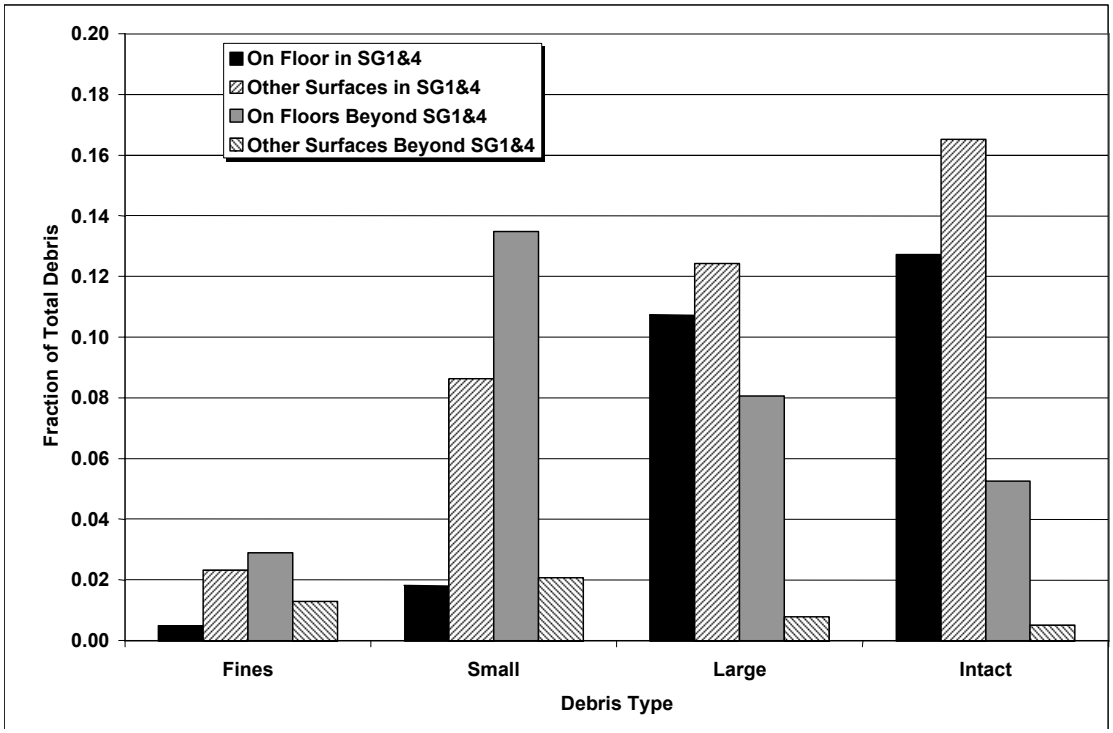

Figure VI-12. Blowdown Debris Dispersion by Surface Orientation

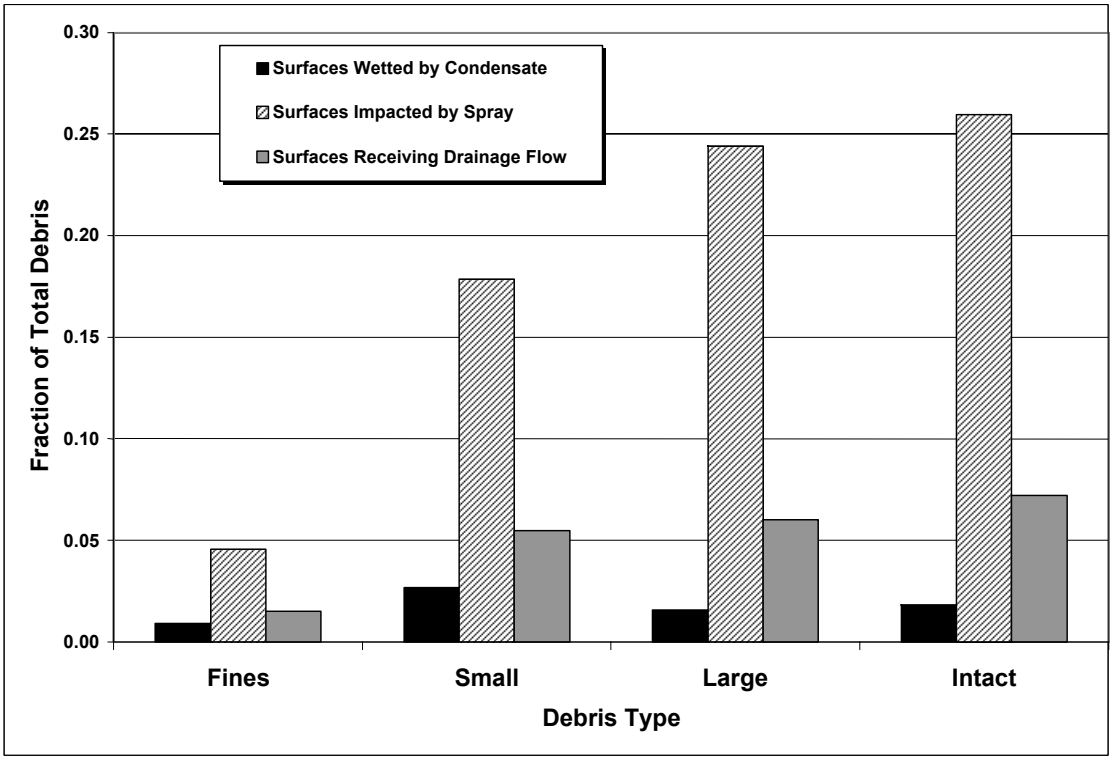

Figure VI-13. Blowdown Debris Dispersion by Surface Wetting

In Figure VI-13, all of the LOCA-generated debris is distributed fractionally according to the surface wetting condition (condensate, sprayed, or spray drainage) and by debris type. Only relatively small quantities of debris were predicted to reside at locations where the CSs or the spray drainage would not wash the debris downward. Conservatively speaking, the sprays falling from the upper dome would wash a majority of the surfaces within the SG compartments, as well as all of the upper floor surfaces and the refueling pool areas.

Although there is a relatively high degree of uncertainty with these blowdown transport results, the trends generally make sense. Because so little debris is protected from the CSs, these trends indicate a relatively high transport of debris to the sump pool.

VI.4.1.2 Fibrous Washdown Debris Transport

The CSs and condensation of steam throughout the containment and subsequent drainage to the sump pool would entrain substantial debris that was deposited onto the various surfaces and would transport the debris to the sump pool. In addition, these processes would degrade the fibrous insulation debris to some extent further, thereby creating more of the very fine, readily transportable debris.

VI.4.1.2.1 Surface Retention of Deposited Debris

The fraction of debris that stays on a specific surface, as opposed to washing away, is referred to as the retention fraction. The fraction transported from a specific surface would then be 1 minus the retention fraction. Estimates of the retention fractions were essentially engineering judgments that were based on experience with small-scale testing during the DDTS. These experiments did not examine specifically the flow requirement needed to remove a piece of debris from a specified type of surface. Most of these tests dealt with either debris generation or airborne debris transport. One set of tests examined the erosion that was associated with fibrous debris inundated by water flow. During the conduct of these tests, experience with the handling of the debris provided some understanding regarding the ease or difficulty of forcing a piece of debris to move. Table VI-15 summarizes these findings. Table VI-16 and Table VI-17 show the estimated transport and corresponding retention fractions, respectively.

Debris transport from condensate drainage would be expected to affect only the smaller debris. As condensation builds on a surface, it forms a thin film that subsequently drains and typically forms small rivulets of flow. This flow usually would move around significantly sized pieces of debris. Individual fibers could be entrained in the flow, or the fiber simply could be pushed to the sides of the rivulets. Some fine and small-piece debris certainly would transport, but the quantities of small debris transporting were estimated to be a small portion of the total. The DDTS's central estimate (realistic yet conservative) assumed that 1 percent of small debris transported (the extreme upper bound was 10 percent) but no large debris. The DDTS did not separate fines from small pieces. For this estimate, increasing the 1 percent to 2 percent for small-piece debris and increasing the 1 percent to 5 percent for the fines increased the level of conservatism. The larger debris was assumed not to transport because of condensate runoff.

Table VI-15. Fibrous-Debris Washdown Transport Trends

Debris Type	Surfaces Wetted by Condensate	Surfaces Either Sprayed or Receiving Drainage Flow	
		Without Intervening Floor Drains	With Intervening Floor Drains
Fines	Minority Transport	Nearly Complete Transport	
Small Pieces	Minority Transport	Majority Transport	
Large Pieces	No Significant Transport	Medium Transport	No Significant Transport
Intact Pieces	No Significant Transport	Minority Transport	No Significant Transport

Table VI-16. Estimated Fibrous-Debris Washdown Transport Percentages

Debris Type	Surfaces Wetted by Condensate	Surfaces Either Sprayed or Receiving Drainage Flow	
		Without Intervening Floor Drains	With Intervening Floor Drains
Fines	5%	99%	
Small Pieces	2%	70%	
Large Pieces	0%	50%	0%
Intact Pieces	0%	20%	0%

Table VI-17. Estimated Fibrous-Debris Washdown Retention Fractions

Debris Type	Surfaces Wetted by Condensate	Surfaces Either Sprayed or Receiving Drainage Flow	
		Without Intervening Floor Drains	With Intervening Floor Drains
Fines	0.95	0.01	
Small Pieces	0.98	0.3	
Large Pieces	1	0.5	1
Intact Pieces	1	0.8	1

Whenever fine and small-piece debris would be subjected to the substantial flows of the impacting CSs or the subsequent drainage of the sprays, the flow likely would entrain nearly all of the fine debris and a majority of the small debris. Test experience indicates that the CSs would wash fines from surfaces easily and carry those fines with the drainage to the sump pool. However, some of this fine debris would be pushed into relatively protected spots, corners, and crevices where the debris would remain. Surfaces that were impacted directly by sprays and drained surfaces were grouped

together for washdown transport because of the lack of information that was required to treat these two surface types differently. It was assumed that 99 percent of the fines would be transported from surfaces that were impacted by the sprays or drainage and that the other 1 percent experienced something less than total transport.

The CSs also would wash substantial small-piece debris off structures, walls, and floors. The DDTS's central estimate was 50 percent (realistic yet conservative), with an extreme upper bound of 100 percent. Substantial quantities of debris likely would become trapped at locations that were protected from full spray flow by the complex arrangements of containment equipment and piping. It was assumed that 70 percent of the small debris would transport from surfaces that were impacted directly either by the CSs or by the subsequent drainage. This assumption adds conservatism to the DDTS's central estimate without becoming excessively conservative.

A simple floor-water drainage calculation, in which a uniform spray was applied to a floor area at a rate of flow corresponding to the containment-dome spray trains A and B, further supported the 70-percent estimate. A floor-area estimate indicates that each floor drain would drain approximately 800 ft^2. A plant calculation estimated that the floor-water holdup depth would be approximately 1.5 in. The separate-effect characterization of debris transport in water tests (NUREG/CR-6772, 2002) shows that a turbulent flow velocity as low as approximately 0.06 ft/s can cause a small piece of debris to tumble or slide along the floor. If circular drainage geometry is assumed, the transport estimate indicates that 30 to 40 percent of the floor area would not have sufficient flow velocity to transport small-piece debris. This calculation did not consider the effect of structures on the transport, which would create locations for debris entrapment. Therefore, the 70-percent estimate is a reasonable number for small-debris transport by the CSs.

For the large and intact pieces of debris, the surfaces were split into two additional categories based on whether the transport of the debris would encounter floor drain holes that would prevent further transport. A typical floor drain is approximately 6 1/2 in. in diameter and has a coarse grating that would stop any debris that is larger than approximately 3 in. square. A few floor drains have a relatively fine mesh screen over the hole. Floor surfaces are sloped to channel water to the drains. Large debris deposited onto the upper floors likely would have to pass through more than one of these floor drains to reach the sump. Large debris settling into the refueling pools would also have to pass through drains to reach the sump, some of which have a screen cover. The two largest of the refueling drains are nominal 6-in. drains without any cover or grating and are open during normal operation. Although a piece of large debris could pass through this 6-in. drain, the amount of debris would not be enough to treat these drains separately. It was assumed that these drains would stop further transport of large and intact debris.

Conversely, large and intact debris that is deposited at locations such as the SG compartments would not encounter any drain holes as the debris transports toward the sump pool. The CSs would wash substantial quantities of large-piece debris off structures, walls, and floors. A portion of the large debris would be trapped on top of gratings and would not transport. Other large pieces would snag onto structures such that the sprays would not dislodge them. Substantial quantities of debris likely would become trapped at locations that are protected from full spray flow by the complexities of containment equipment and piping. Because large debris would transport less easily than small debris, it was assumed that 50 percent of the large debris was transported.

The intact debris would be less likely to transport than the large-piece debris. Based on DDTS experience, the intact pieces of debris were significantly more likely to snag on structures than the large pieces, and substantial quantities of intact debris were likely to remain attached to the original piping. It was assumed that 20 percent of the intact debris would transport.

VI.4.1.2.2 Erosion of Debris by CSs

Experiments conducted in support of the DDTS analysis illustrated that the flow of water could further erode insulation debris. Some debris erosion could occur because of the impact of the sprays and spray drainage flows, but the amount of erosion would not be great. The DDTS concluded that less than 1 percent of the fibrous debris eroded as a result of CS operation. The analysis neglected debris erosion caused by condensation and condensate flow. Debris containing insulation that is still in its cover would not be expected to erode further. The sump-pool transport analysis includes the erosion of debris caused by the plummeting of the break flow into the sump pool.

It was assumed that condensate drainage would not cause further erosion of fibrous debris and that intact or covered debris would not erode further. Erosion does not apply to fine debris because the debris is already fine. It was assumed that 1 percent of the small- and large-piece debris that was impacted directly by the sprays would erode, and that intact pieces of debris could not erode because its canvas cover would protect the fibrous materials.

VI.4.1.3 Quantification of Fibrous-Debris Transport

The transport of fibrous debris was quantified using the models presented in Section VI.3 and the input presented in Section VI.4.1. Table VI-18 presents the quantified transport results and shows the transport fractions for each size category, as well as the overall transport fraction. It also shows the fractions of the total ZOI insulation that entered the pool, which were normalized to provide a size distribution for the debris entering the pool. About 57 percent of the ZOI fibrous insulation was predicted to transport to the sump pool, and nearly half of that would be the relatively transportable sizes. The transport fraction for the fines includes the erosion products from the predicted erosion of the small and large pieces of debris. The quantity of erosion products was approximately equal to 6 percent of the original generated fines.

Table VI-18. Fibrous-Debris-Transport Results

Debris Size Category	Category Generation Fraction	Size Category Transport Fraction	Fraction of ZOI Insulation	Distribution Entering Sump Pool
Fines	0.07	0.93	0.07	0.12
Small Pieces	0.26	0.66	0.17	0.30
Large Pieces	0.32	0.54	0.17	0.30
Intact Pieces	0.35	0.46	0.16	0.28
All Debris	1.00	0.57	0.57	1.00

VI.4.2 RMI Debris Transport

Roughly 85.7 percent of the insulation in the volunteer-plant containment is RMI. The debris-transport methodology discussed in Section VI.3 applies to RMI debris, as well as fibrous debris. Unfortunately, unlike the fibrous insulation, very little useful airborne transport data for RMI debris exist. Specifically, the capture fractions for the capture of RMI debris passing through structures such as gratings and of RMI debris inertially impacting surfaces have not been measured. Only secondary experience associated with RMI debris-generation experiments applies in this study. For RMI debris washdown, the pool transport velocities are available. Small-scale experiments suggest that RMI debris transports less easily than the fibrous debris, primarily because the RMI debris is heavier. In addition, it would take substantially more RMI debris on the sump screen than fibrous debris to block flow effectively through the screen.

VI.4.2.1 RMI Blowdown Debris Transport

The capture fractions for RMI debris are likely much different from the corresponding fractions for fibrous debris. For fibrous debris, the capture fractions were very dependent on surface wetting; when the surfaces were dry, debris capture was minimal. For RMI, surface wetting may not be important. For instance, it seems likely that the capture of RMI on a grating depends on the foil folding over a bar in such a manner that it remains in place. Capture may depend on the debris remaining stuck on a structure. The amount of RMI debris that was captured by a grating could be significantly less than the amount of fibrous insulation; conversely, it could be substantially more. Furthermore, the ability of flows to transport large cassette-like RMI debris is not known. Therefore, application of the Section VI.3 methodology required very conservative assumptions to compensate for the nearly complete lack of data.

VI.4.2.1.1 Break-Region Blowdown Debris Transport

It is conservative to overestimate the retention of debris within the SG compartments because subsequent debris washdown is more likely if the debris were in the SGs as opposed to dispersed throughout the containment. Because the capture rates for RMI debris passing through a grating have not been determined, it was conservatively assumed that the grating stopped 100 percent of all RMI debris impacting it from further forward transport. Debris stopped on the underside of a grating likely could fall back once depressurization flows subside. Because the gratings do not extend completely across the SG compartments, substantial debris still could be propelled upward into the containment dome.

Likewise, the inertial capture of RMI debris by miscellaneous structures (e.g., pipes, beams, or vessels) or by inertial impaction whenever the flow makes a sharp bend has not been determined. For instance, it would seem less likely that a piece of RMI debris would stick to a wall than would a small piece of fibrous debris. The fibrous-debris capture fractions for miscellaneous structures and sharp bends were applied to the RMI debris to conservatively overpredict the retention of RMI debris within the SG compartments. Applying these assumptions to the logic charts, which are similar to Figure VI-7, results in the conservative SG capture fractions shown in Table VI-19. The values for 2- to 6-in. and the larger-than-6-in. debris categories in Table VI-19 correspond to the values for the fibrous large- and intact-category values (shown in Table VI-11) a result of similar assumptions. The assumption that the gratings capture

all of the RMI debris, even the smallest pieces, predicts substantially more RMI retention within the SG compartments than likely would occur in reality. The lack of RMI transport data necessitated the predicted overconservative retention.

Table VI-19. Fractional Distribution of Debris Captured and Exiting Break Region

Location	RMI Debris Category		
	<2-in. Pieces	2- to 6-in. Pieces	>6-in. Pieces
Captured within SGs 1 and 4	0.64	0.70	0.82
Expelled to Dome	0.32	0.26	0.17
Expelled to Level 832	0.01	0	0
Expelled to Level 808	0.03	0.04	0.01

VI.4.2.1.2 Dispersion throughout the Remainder of Containment

The RMI debris-transport estimate employed the same 24-region subdivision of the containment free volume that was used in the fibrous-debris-transport estimate (Table VI-12). The volume weighting factors that were estimated for fibrous-debris transport (Table VI-13) also were applied to the RMI debris because no rationale was found to weight the distributions otherwise. For RMI debris, no fine debris was postulated (i.e., even the smaller pieces of RMI debris should sink readily in water, as opposed to fibrous fines, which tend to remain in suspension). The predicted dispersion of RMI debris was judged to place more debris into locations where it subsequently would be predicted to transport with the CS drainage to the sump pool. Table VI-14 illustrates the results of the blowdown dispersion by groups of volume regions. As modeled, the break region (SGs 1 and 4) retained a majority of the debris. In reality, it is likely that much more of the smaller debris would be blown free of the break region and into the upper dome region, where subsequent washdown to the sump pool would be substantially less than it would be if the debris were kept within the break region. However, the lack of RMI debris-transport data necessitated the conservative assumptions leading to these results.

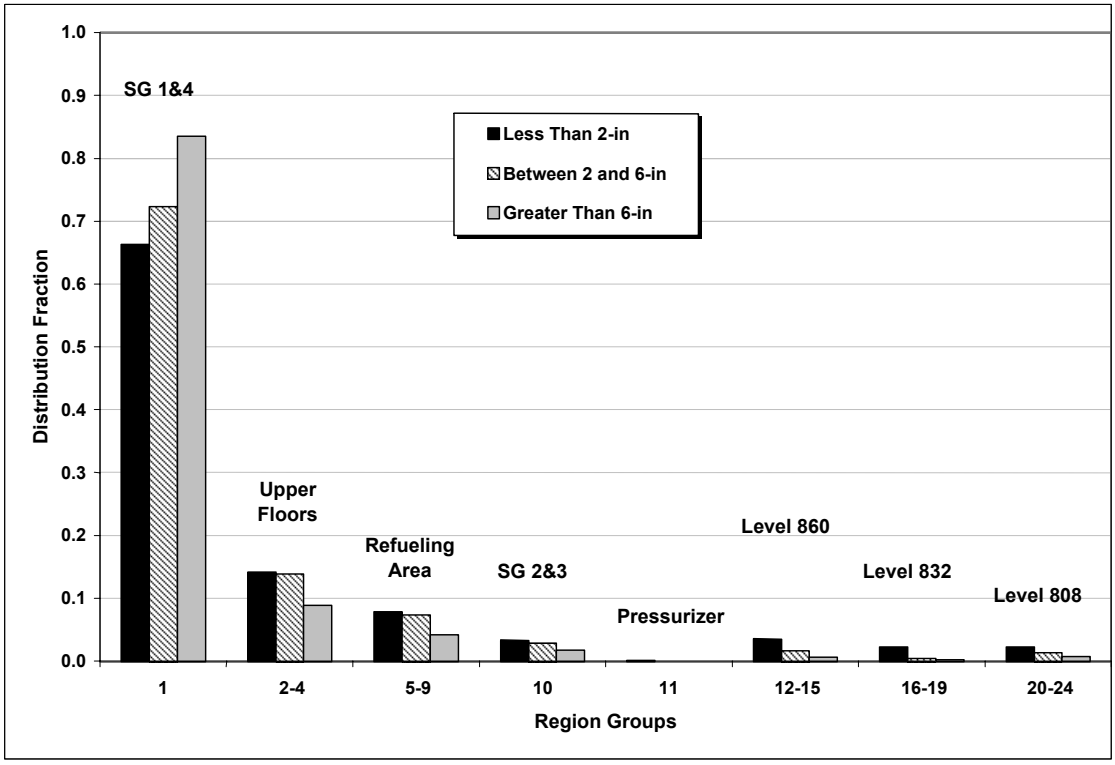

Figure VI-14. RMI Blowdown Distribution by Region Groups

VI.4.2.1.3 Dispersion by Surface Orientation and Surface Wetness

A review of photos that were taken of RMI debris following RMI debris-generation tests indicates that RMI debris would reside preferentially on the floor surfaces (NEDO-32686, 1996; LA-UR-01-1595, 2001), although some RMI debris was caught on structures. However, the structures in these debris-generation tests were dry; therefore, it is not known if surface wetness would cause RMI to stick to wetted surfaces. Still, it is conservative to place the debris on the floors, where the subsequent washdown would be more effective. Therefore, the various surface-area-weighting factors were set to place most of the RMI debris on the volume region floors. It was assumed that 99 percent of the RMI debris would reside on the floor. The surface-area fractions shown in Table VI-14 apply to RMI debris as well as to fibrous debris. In these assumptions, approximately 99 percent of the RMI debris following blowdown was located where it either was impacted directly by the sprays or was located in the path of the spray drainage, leaving only 1 percent on surfaces that were wetted by condensation only.

VI.4.2.2 RMI Washdown Debris Transport

The RMI debris surface-retention fractions (i.e., the fraction that was not washed away) were estimated based primarily on engineering judgments and RMI pool debris-transport data. Small-scale testing of the transport of RMI debris in a pool of water demonstrated the ease or difficulty of forcing a piece of debris to move in a pool of water. Debris transport in a flowing layer of water that resides on a floor is similar to the transport of the debris in an established pool of water. Table VI-20 summarizes perceptions

regarding the transport of RMI debris in nonpool situations. Table VI-21 and Table VI-22 show the estimated transport and corresponding retention fractions, respectively.

Table VI-20. RMI-Debris-Washdown Transport Trends

Debris Type	Surfaces Wetted by Condensate	Surfaces Either Sprayed or Receiving Drainage Flow	
		Without Intervening Floor Drains	With Intervening Floor Drains
<2 in.	Minority Transport	Medium Transport	
2 to 6 in.	No Significant Transport	Medium Transport	No Significant Transport
>6 in.	No Significant Transport	Minority Transport	No Significant Transport

Table VI-21. Estimated RMI-Debris-Washdown Transport Percentages

Debris Type	Surfaces Wetted by Condensate	Surfaces Either Sprayed or Receiving Drainage Flow	
		Without Intervening Floor Drains	With Intervening Floor Drains
<2 in.	1%	40%	
2 to 6 in.	0%	30%	0%
>6 in.	0%	10%	0%

Table VI-22. Estimated RMI-Debris-Washdown Retention Percentages

Debris Type	Surfaces Wetted by Condensate	Surfaces Either Sprayed or Receiving Drainage Flow	
		Without Intervening Floor Drains	With Intervening Floor Drains
<2 in.	99%	60%	
2 to 6 in.	1%	70%	1%
>6 in.	1%	90%	1%

All debris that was deposited onto the SG compartment floors and the sump-level floors automatically was assumed to have entered the sump pool; the tables do not indicate this assumption. This assumption primarily affected the debris that was deposited onto the break-region floor during either blowdown or washdown. The falling and spreading

break flow would drive the actual movement of this debris from the SG compartment floor into the outer annulus; this would generally be expected to result in a relatively high level of transport.

Debris transport resulting from condensate drainage would be expected to affect only the smaller debris. As condensation builds on a surface, it forms a thin film that subsequently drains and typically forms small rivulets of flow. This flow usually would not move around significantly sized pieces of debris. Significant transport of RMI debris does not seem likely; however, it is possible that some of the smaller debris could move with the condensate flow until the condensate flow linked up with more substantial water drainage. It was assumed that 1 percent of the debris that was less than 2 in. and subjected only to condensate drainage ultimately would transport to the sump pool. Furthermore, it was assumed that none of the debris that was greater than 2 in. would transport to the sump pool.

Whenever pieces of debris less than 2 in. were subjected to substantial flows from the CSs or from the subsequent drainage of the sprays, the flow likely would entrain a substantial portion of that debris. The evaluation of the transport of the smaller RMI debris that was exposed to sprays and/or spray drainage was based on a floor-pool drain velocity estimate and on the pool debris-transport threshold velocities. The drainage-flow velocity calculation assumed that a uniform spray was applied to an upper level floor area corresponding to the containment-dome spray trains A and B. A floor-area estimate indicated that each floor drain would drain approximately 800 ft^2 of floor area. A plant calculation estimated a floor-water holdup depth of approximately 1.5 in. The separate-effect characterization of debris transport in water tests (NUREG/CR-6772, 2002) showed that a turbulent flow velocity of approximately 0.2 ft/s would be required to cause small stainless-steel RMI debris to tumble or slide along the floor. If it is assumed that circular drainage geometry exists, the transport estimate indicates that 60 to 80 percent of the floor area would not have sufficient flow velocity to transport small stainless-steel RMI debris, depending on the assumed thickness of the water layer. This conclusion resulted in the 40-percent transport estimate shown in Table VI-21. Because this calculation did not consider the effect of structures on the transport, which would create locations for debris entrapment, the 40-percent transport estimate is a reasonable number for the transport by the CSs of RMI debris that is less than 2 in.

As was done for fibrous debris, pieces of RMI debris that were greater than 2 in. were assumed not to pass through floor drains or refueling-pool drains. At locations where the larger debris would not encounter floor or refueling drains, 30 percent of the 2- to 6-in. debris and 10 percent of the debris that was greater than 6 in. were assumed to transport. The corresponding fibrous-debris-transport number simply was reduced based on engineering judgment to account for the fact the RMI debris transports less easily than does fibrous debris. In any case, these two estimates affected only a relatively minor portion of the total debris.

Debris erosion of any significance would not happen to stainless-steel RMI debris; therefore, this study did not consider the erosion of the RMI debris by the CSs.

VI.4.2.3 Quantification of RMI Debris Transport

The transport of fibrous debris was quantified using the models presented in Section VI.3 and the input presented in Section VI.4.2. Table VI-23 presents the quantified

transport results. The table shows the transport fractions for each size category, as well as the overall transport fraction. It also shows the fractions of the total ZOI insulation that entered the pool. These fractions then were normalized to provide a size distribution for the debris entering the pool. Approximately 83 percent of the ZOI RMI was predicted to transport to the sump pool, but only approximately 20 percent of that amount was pieces less than 2 in.

Table VI-23. Fractional RMI Debris-Transport Results

Debris-Size Category	Category Generation Fraction	Size Category Transport Fraction	Fraction of ZOI Insulation	Distribution Entering Sump Pool
<2 in.	0.21	0.82	0.17	0.21
2 to 6 in.	0.12	0.76	0.09	0.11
>6 in.	0.67	0.85	0.57	0.68
All Debris	1.00	0.83	0.83	1.00

VI.4.3 Min-K Insulation Debris Transport

Less than 1 percent of the insulation in the volunteer-plant containment is Min-K insulation, a form of insulation referred to as microporous or particulate insulation. Although the transport methodology discussed in Section VI.3 also applies to Min-K insulation, a nearly complete lack of airborne transport data for this type of insulation exists, as well as debris-generation data, which were discussed in Section VI.3.2.3. Because of the lack of data for the generation of debris from Min-K insulation, the unknown erosion characteristics of this insulation, and the sparseness of the insulation within the containment (i.e., leads to a potential spatial nonuniform distribution), it was conservatively assumed that all Min-K located within the ZOI would be pulverized into a fine, highly transportable dust. If the CSs inundated the larger pieces of Min-K debris, these pieces simply could dissolve into fine silt and transport with the spray drainage; however, this outcome is yet to be proven. Although less than 1 percent of the containment insulation is Min-K, this type of particulate debris could affect the sump-screen head losses significantly.

A conservative transport fraction for Min-K dust must be relatively high, and it seems likely that this fraction would be similar to the fraction for the transport of fibrous fines without the addition of erosion products, which was approximately 0.87. That is, the transport of fibrous fines generated from the ZOI to the sump pool was approximately 87 percent. (Note that the 93 percent value that was shown in Table VI-18 included erosion products.) Because the bulk of the 13 percent of fine fibers that did not transport was located on surfaces wetted only by condensate, it seems likely that a similar result would occur for the Min-K. This study assumed that 90 percent of the Min-K dust would transport to the sump pool.

VI.5 Blowdown/Washdown Conclusion

A methodology was developed that considers both transport phenomenology and plant features. It divides the overall complex transport problem into many smaller problems that either are amenable to solution by combining experimental data with analysis or that can be judged conservatively based on the foundation of debris-transport knowledge. The quantification of the methodology results in predicted transport fractions that are both conservative and plausible. Table VI-24 shows the overall transport results. These transport fractions represent the fractions of the insulation by type that was initially located within the ZOI and that subsequently would transport to the sump pool. Sections VI.3 and VI.4 discuss the detailed results, including size distribution information.

Table VI-24. Overall Transport Results

Insulation Type	Overall Transport Fraction*	Debris-Size Distribution
Fibrous	57%	Table VI-18
RMI	83%	Table VI-23
Min-K	90%	All Dust

* Overall percentages are for demonstration only.

The overall transport fractions listed in Table VI-24 serve for demonstration purposes but are not valid for plant-specific evaluations because these fractions were calculated using LOCA-generated debris-size distributions that did not account properly for PWR jet characteristics. The BWR jet characteristics were substituted for PWR jet characteristics because the PWR jet analyses had not been performed yet. When the PWR jet characteristics become available, it will be a simple matter to recalculate the overall transport fractions using PWR LOCA-generated debris-size characteristics.

Neither the debris-size distributions nor the overall transport fractions in this report are valid for plant-specific evaluations.

The transport fractions for each debris-size category are considered to be conservative for the LDFG insulation in the volunteer plant (but not necessarily for containments of other design). The fibrous-debris-transport analysis contained herein was based on LDFG insulation and may require adjusting for any high-density fiberglass insulation or mineral wool that may also be in the plant.

For the volunteer plant, a high percentage of the fine LOCA-generated debris most likely would transport to the sump pool via the spray drainage flows. The transport fractions tended to decrease as the debris size increased. A majority of the larger debris that was predicted to transport to the sump pool was stopped in the SG compartments that were associated with the break, where subsequent CS drainage was assumed to be readily capable of moving the debris downward to the pool.

The lack of transport data caused the transport of the RMI and Min-K debris to skew more conservatively toward larger transport fractions than the fibrous debris. Realistically speaking, the RMI might be expected to transport less readily than would the fibrous debris because it is heavier. However, a larger fraction of the RMI debris could be trapped in the break region (SG compartments), where it could be transported subsequently into the sump pool, and thus the need to skew the transport fractions conservatively. A similar discussion applies to the Min-K because of the lack of LOCA debris-generation data, lack of erosion data, and the potential nonuniform placement of Min-K in the ZOI. Therefore, most of the Min-K must be conservatively assumed to transport to the sump pool as a fine dust or silt.

This analysis used conservative engineering judgments at various steps along the way. The degree of conservatism that was associated with these judgments was intended to ensure conservative final results without straying too far from realistic behavior. The judgments were not intended to be upper bounding. For example, the DDTS assessed the erosion of LDFG by CSs as less than 1 percent. In reality, the erosion may be significantly less than 1 percent. The 1 percent value was assumed to be conservative but not far from reality. In addition, many conservative judgments tend to compound as the analysis progresses.

The analyses herein considered only one break location (SG1), although they included a range of break sizes at that location. Plant-specific analyses must consider a range of break locations. For the volunteer plant, LOCAs can occur within an SG compartment, which is likely the most probable location. A break in the same SG but at a different level likely would have a result similar to the one analyzed because most of the break effluent still would flow to the containment dome. A break in an SG compartment different from SG1 most likely would have a similar result, except that the debris would tend to enter the sump pool at different locations. A break outside the SG compartments, such as in a main steamline, would behave differently than a break inside an SG compartment and probably should be analyzed separately. A break in the pressurizer certainly would be different because that compartment does not vent directly to the containment dome as do the SG compartments (i.e., no major upper openings exist). Therefore, a larger fraction of the debris might be driven out of the pressurizer compartment directly into the sump area, but the total quantity of debris might be substantially less than a primary-loop piping break. This discussion does not analyze either a pressurizer-line break or a main steamline break.

In performing blowdown/washdown analyses, it is important to ensure the following:

- The debris-size categories match the characteristics of the debris-transport behavior.
- The break region is analyzed in substantial detail because so much of the debris capture is likely to occur in this region.
- The debris capture along the primary exits from the break region also should be analyzed in substantial detail.
- The CS drainage patterns should be determined to support the washdown analysis and to indicate where the debris would enter the sump pool and how the spray drainage would impact sump pool turbulence.

- Vulnerable spray-drainage pathways, where potential debris blockage might occur, should be identified.

VI.6 References

(LA-UR-99-3371, 1999) Boyack, B.E., et al., "PWR Debris Transport in Dry Ambient Containments—Phenomena Identification and Ranking Tables (PIRTs)," LA-UR-99-3371, Revision 2, December 14, 1999.

(LA-UR-01-1595, 2001) Rao, D.V., C.J. Shaffer, and R. Elliott, "BWR ECCS Strainer Blockage Issue: Summary of Research and Resolution Actions," prepared for the U.S. Nuclear Regulatory Commission by Los Alamos National Laboratory, LA-UR-01-1595, March 21, 2001.

(NEDO-32686, 1996) "Utility Resolution Guidance for ECCS Suction Strainer Blockage," BWROG, NEDO-32686, Rev. 0, November 1996.

(NRC-SER-URG, 1998) "Safety Evaluation by the Office of Nuclear Reactor Regulation Related to NRC Bulletin 96-03 Boiling Water Reactor Owners Group Topical Report NEDO-32686, 'Utility Resolution Guidance for ECCS Suction Strainer Blockage,'" Docket No. PROJ0691, August 20, 1998.

(NUREG/CR-6369-1, 1999) Rao, D.V., C. Shaffer, and E. Haskin, "Drywell Debris Transport Study," NUREG/CR-6369, Volume 1, SEA97-3501-A:14, September 1999.

(NUREG/CR-6369-2, 1999) Rao, D.V., et al., "Drywell Debris Transport Study: Experimental Work," NUREG/CR-6369, Volume 2, SEA97-3501-A:15, September 1999.

(NUREG/CR-6369-3, 1999) Shaffer, C.J., D.V. Rao, and J. Brideau, "Drywell Debris Transport Study: Computational Work," NUREG/CR-6369, Volume 3, SEA97-3501-A:17, September 1999.

(NUREG/CR-6762, Vol. 1, 2002) Rao, D.V., et al., "GSI-191 Technical Assessment: Parametric Evaluations for Pressurized Water Reactor Recirculation Sump Performance," LA-UR-01-4083, Los Alamos National Laboratory, August 2002.

(NUREG/CR-6762, Vol. 2, 2002) Rao, D.V., et al., "GSI-191 Technical Assessment: Summary and Analysis of U.S. Pressurized Water Reactor Industry Survey Response and Responses to GL 97-04," Volume 2, LA-UR-01-1800, Los Alamos National Laboratory, August 2002.

(NUREG/CR-6762, Vol. 3, 2002) Rao, D.V., C.J. Shaffer, and S.G. Ashbaugh, "GSI-191 Technical Assessment: Development of Debris-Generation Quantities in Support of the Parametric Evaluation," LA-UR-01-6640, Los Alamos National Laboratory, August 2002.

(NUREG/CR-6772, 2002) Rao, D.V., B.C. Letellier, A.K. Maji, and B. Marshall, "GSI-191: Separate-Effects Characterization of Debris Transport in Water," NUREG/CR-6772, LA-UR-01-6882, August 2002.

(NUREG/CR-6773, 2002) Rao, et al., “GSI-191: Integrated Debris-Transport Tests in Water Using Simulated Containment Floor Geometries,” NUREG/CR-6773, LA-UR-02-6786, December 2002.

(NUREG/CR-6808, 2003) Shaffer, C.J., D.V. Rao, M.T. Leonard, and K.W. Ross, “Knowledge Base for the Effect of Debris on Pressurized Water Reactor Emergency Core Cooling Sump Performance,” NUREG/CR-6808, LA-UR-03-0880, February 2003.

(OPG, 2001) Russell, J., “Jet Impact Tests—Preliminary Results and Their Application,” N-REP-34320-10000, Rev. R00, April 18, 2001.

(SEA-95-970-01-A:2, 1996) Zigler, G., et al., “Experimental Investigation of Head Loss and Sedimentation Characteristics of Reflective Metallic Insulation Debris,” draft letter report, prepared for the U.S. Nuclear Regulatory Commission, SEA No. 95-970-01-A:2, May 1996.

ATTACHMENT 1 TO APPENDIX VI

VOLUNTEER-PLANT SPRAY-WATER DRAINAGE ANALYSIS

1. Introduction

A postulated LOCA in the volunteer plant would distribute insulation debris throughout the containment, whereby the subsequent drainage of spray water following the LOCA would transport portions of this insulation debris toward the recirculation sump screens. A best estimate of how the water would drain to the sump was performed to support subsequent debris-transport calculations. The analysis will help to identify spaces and surfaces where sprays or drainage flow would not likely wash away insulation debris (e.g., an area that was not impacted by sprays and has too little drainage flow to transport debris). The analysis will help to determine how the drainage water enters the sump pool, which in turn will affect debris transport within that pool.

2. System Descriptions

The CS systems in the volunteer plant consist of two independent trains (trains A and B), with headers located in four containment regions. Spray nozzles are located in one of four regions of the containment:

- Region A—containment dome spraying down toward Level 905
- Region B—below Level 905 spraying Level 860
- Region C—below Level 860 spraying Level 832
- Region D—below Level 832 spraying Level 808

Table 1 shows the specifications for both trains in Unit 1, combined. Spray train B has one more nozzle in the dome than train A; therefore, the flows that are associated with single train operations constitute essentially half of the flows shown for both trains. Unit 1 has seven more nozzles than Unit 2. The drainage estimate performed for Unit 1 applies also to Unit 2.

Table 1. Unit 1 Spray Nozzle Summary

Spray Region	Number of Nozzles	Nozzle Flow (gpm)	Region Flow (gpm)
A	545	20	10,900
B	134	20	2,680
C	28	20	560
D	54	20	1,080
Total	761	20	15,220

The containment was designed to drain the spray water down to the containment recirculation sumps. Furthermore, the containment apparently was designed to

minimize water holdup, thereby maximizing the depth of the sump pool. Several features of the containment, including those described below, determine the primary drainage pathways in the containment.

Floor drains that drain water from one floor directly down to the next floor are a primary means of draining spray water. Figure 1 shows a typical drain, which is approximately 6.5 in. in diameter. At the top of this figure, another type of drain leads directly to the containment sump. Floor surfaces are sloped to channel water into the drains.

Figure 1. Typical Floor Drain

Water barriers (curbs), both concrete and metallic types, control water drainage. These barriers are placed around floor-area perimeters to prevent water from draining from those perimeters. However, these barriers do not cover the entire perimeter of a floor. Gaps exist in the barriers at locations such as the areas around walkways and ladders. In many places, water can flow from a floor perimeter onto another floor, into the gap between the internal structures and the outer wall, into an SG compartment, or into a stairwell. Figure 2 shows a typical curb. Figure 3 shows another curb next to an SG compartment that illustrates a discontinuity in a curb.

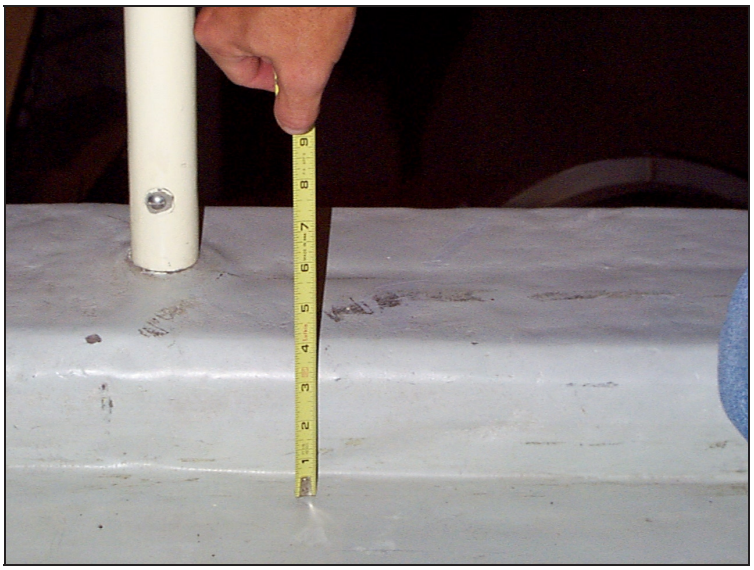

Figure 2. Typical Concrete Curb

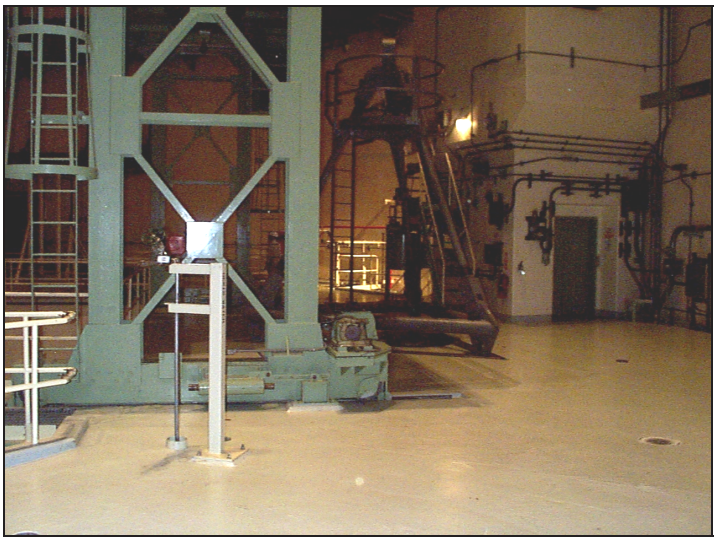

Figure 3. Gap in Concrete Curb Surrounding an SG Compartment

A substantial portion of the dome sprays will fall into the refueling cavity and accumulate in the three pool areas of the cavity. During normal operation, the pool drains are open, allowing spray water to drain down to the sump. The pool drains consist of 4-in. and 6-in. sizes. Figure 4 shows the drains in the pool that are used to store the reactor vessel lower internals during refueling. Near the center, the photo shows a 4-in. drain with a cover screen (with holes approximately 1/4 to 1/2 in. in diameter). In the upper-right (cover off) and lower-right corners (cover in place), the photo also shows two 6-in. drains. These 6-in. drains are closed off with blind flanges during refueling and are uncovered during normal operations. The 4-in. drains lead down into the labyrinth of rooms on Level 808, which is located directly below the refueling pools. The two 6-in. drains flow to SGs 3 and 4. A single 4-in. drain draws off the pool that is used to store and transfer fuel to Level 808. The pool that is used to store reactor vessel upper

internals during refueling has a single 4-in. drain, which drains into the pool that stores the lower internals.

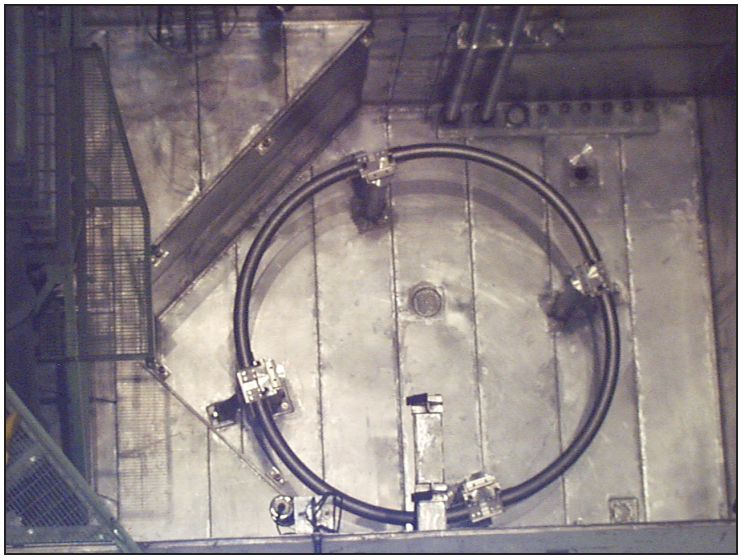

Figure 4. Refueling Pool Drains

Water drainage between floors also occurs through the floor gratings that cover several open areas in the floors (e.g., the equipment-transfer floor hatches).

At several staircases, water can drain through stairwells from one floor to the next. Two primary staircases extend all the way from sump Level 808 up to the top floor at Level 905.

3. Approach

A review of containment drawings and plant documents led to many general observations:*

- Little, if any, water is expected to drain down the elevator shaft by way of the elevator doors. The plant's minimum pool calculation did not treat the elevator shaft as a wetted drain perimeter, and the floors generally slope away from elevator. Furthermore, elevator doors may prevent water entry into the elevator shaft.
- The pressurizer compartment should remain essentially dry. A roof covers the compartment so that sprays do not enter this compartment. Drains and sloping floors generally prevent water flow into this compartment at other entrances.
- Water entering the SG compartments consists of dome-spray droplets falling directly into those compartments. Droplets falling onto the wall-tops and floor that are located between or near the SG compartments likely will flow into the

*The most useful drawings were floor layouts that showed floor slopes, water barriers, and floor drains. The most useful document was a plant calculation of the minimum sump-pool height.

SG compartments. In addition, the two 6-in. refueling-pool drains flow directly into the SG compartments.

- Water entering the stairwells consists of spray droplets falling directly into stairwells and of some water overflowing a floor perimeter.
- Water entering the refueling cavity consists of spray droplets falling directly into the cavity. This water includes droplets that are falling onto walkways surrounding the refueling pool and that subsequently would flow into the pool.
- Water entering the gap between the inner containment structure and the containment outer wall consists of spray droplets impinging the outer containment wall and subsequently flowing down the liner and of water from gaps in the water barriers along the floor perimeters.
- Floor drains between the floors are intended to drain substantial quantities of water from one floor to the next.

Because of the complexity of the water drainage, many simplifying assumptions and engineering judgments were necessary. The primary assumptions include the following:

- All spray systems were active (only one possible spray scenario was evaluated).*
- No blockage of drain flows by debris was postulated.†
- Dome spray droplets fall vertically and distribute uniformly across the containment cross section before encountering any containment structure. Distribution was based on cross-sectional areas.
- Crosswalks on Level 905 that are directly between the refueling cavity and the SG compartments drain into those compartments.
- Refueling cavity walkways on Level 860 drain into pools.
- Levels 873 and 851 do not have floor drains (i.e., floor drains not shown in drawing).
- Water draining onto Level 849 from Level 860 subsequently draws off to Level 832.
- Water drains that lead directly to a containment sump (e.g., the one shown in the upper portion of Figure 1) are neglected. The drawings do not delineate these specialized drains assumed to be substantially fewer in number than the main floor drains.

Engineering judgments were necessary where insufficient data were available to estimate drainage accurately.

---

*The scenario where one train operates and one train is inactive can be estimated by dividing all flows for both trains by a factor of 2.

†Insulation debris could block a floor drain or a refueling pool drain.

The calculational approach included the following steps:

- The locations of all spray nozzles were identified.
- The dome spray impacting and running down the containment liner was estimated.
- The main floor areas on Levels 808, 832, 860, and 905 were nodalized into three sections for each floor.
- The locations where the spray droplets would settle were identified.
- The drainage process was tracked from the uppermost surfaces down to Level 808.

The dome spray nozzles, arranged around four rings for each of the two trains, are aimed in four different directions. Some of the nozzles apparently are aimed to spray the dome liner. A portion of this spray impacting the liner subsequently should drain down the liner itself. The number of nozzles aimed in each of the four directions was tabulated for each ring. Then the spray impact and runoff was judged for each ring location. Of the 10,900-gpm total dome spray flow, 700 gpm was estimated to flow down the liner.

Figure 5 illustrates the subdivision of the main floors. Section 1 includes the side of the containment where the main steam and feedwater lines penetrate the containment. Drainage on this side would be distinctly different from the remainder of the containment. Section 2 includes unique features such as Level 849 and Level 832; sprays do not extend into this section. Section 3 includes the remainder of the floors.

To estimate the distribution of settled dome spray water, the containment cross-sectional area was estimated for each section of floor, refueling cavity, SG compartment, open area, and other areas. It was assumed that the spray droplets would fall uniformly onto these areas. Once the settled flows were determined, the drainage from floor to floor was estimated, starting with the uppermost floor surface. For each floor section, a drainage distribution was estimated, based on floor sloping relative to drainage pathways.

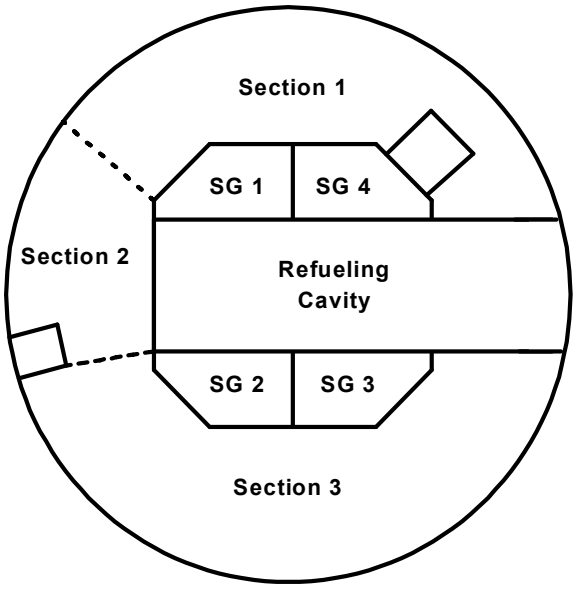

Figure 5. Schematic of Floor Sections

Figure 6 shows the overall spray drainage. The dashed lines represent spray droplets falling onto a surface* (the arrow head indicates the surface receiving the droplets). The numbers indicate flow rates in gallons per minute. The solid lines indicate water draining from one surface to another or water falling into and through a stairwell or the outer wall gap. Figure 7 shows a diagram illustrating where the water enters the Level 808 sump pool.

* The surfaces are not drawn to scale.

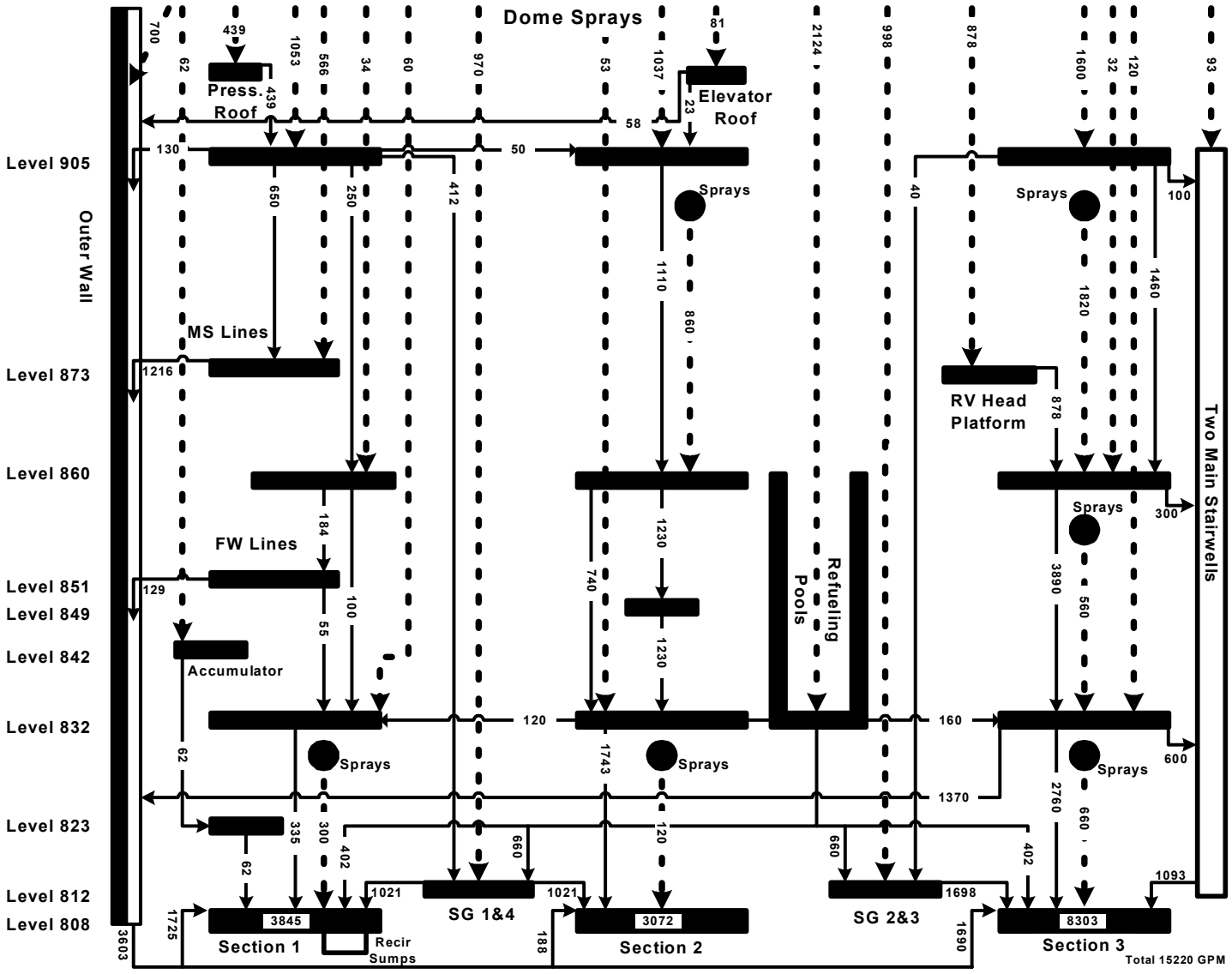

Figure 6. Spray-Water Drainage Schematic

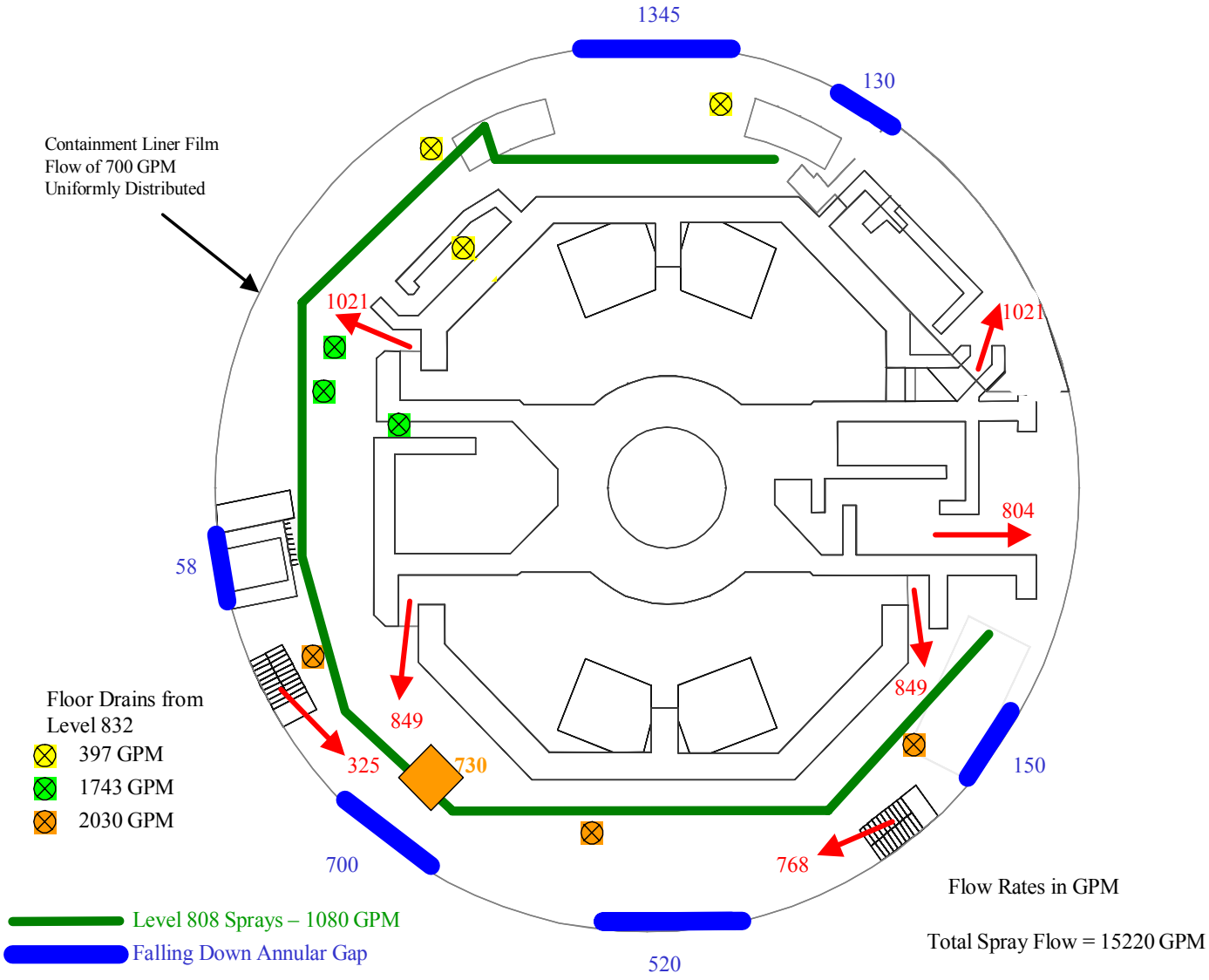

Figure 7. Spray-Water Drainage to Level 808 Sump Pool